AD

USAAVLABS TECHNICAL REPORT 64-68I

HEAVY-LIFT TIP TURBOJET ROTOR SYSTEM
VOLUME IX
PERFORMANCE ANALYSIS

October 1965

U. S. ARMY AVIATION MATERIEL LABORATORIES
FORT EUSTIS, VIRGINIA

CONTRACT DA 44-177-AMC-25(T)

HILLER AIRCRAFT COMPANY, INC.

Task 1M121401D14412
Contract DA 44-177-AMC-25(T)
USAAVLABS Technical Report 64-68I
October 1965

HEAVY-LIFT TIP TURBOJET ROTOR SYSTEM

VOLUME IX

PERFORMANCE ANALYSIS

Hiller Engineering Report No. 64-49

Prepared by

Hiller Aircraft Company, Inc.
Subsidiary of Fairchild Hiller Corporation
Palo Alto, California

For

U. S. ARMY AVIATION MATERIEL LABORATORIES
FORT EUSTIS, VIRGINIA

(U. S. Army Transportation Research Command when report prepared)

CONTENTS

ILLUSTRATIONS

ILLUSTRATIONS (CONTINUED)

ILLUSTRATIONS (CONTINUED)

SYMBOLS

A_b	Total actual blade area
A_I	Total compressor inlet area
A_π	Equivalent flat plate area (C_D = 1.0)
$A_{\pi_{E.L.}}$	Value of A_π at which particular design would be power limited
a'	Slope of C_L of nacelle versus yaw angle, ϕ, where C_L is based on projected nacelle side area, per radian/
a_I'	Same as a' except C_L is based on inlet area
AR_b	Blade aspect ratio (R/chord)
B	Tip loss factor
b	Number of blades
C_D	Drag coefficient
C_L	Lift coefficient
$C_{L_{r_o}}$	Design (sea level) mean rotor lift coefficient
℄	Centerline
F_n	Net thrust
F_R	Total rated thrust
F.L.	Fixed losses
ihp	Induced horsepower
K_u	Inflow correction factor
K_μ	Profile power correction factor for forward speed
ℓ_F	$\dfrac{\text{Rated thrust (total)}}{W_G}$
$MRTHP_{700}$	Military rated thrust horsepower
n	Load factor
n_e	Number of engines

php	Parasite drag horsepower
R	Rotor radius from rotor centerline to centerline of outboard engines
$R_{F_{avail}}$	Fuel weight to gross weight ratio available
R_{hp}	Rotor profile horsepower
SL	Sea level
T_{amb}	Ambient temperature
V_T	Tip Speed
V_{T_H}	Hover tip speed at centerline of outboard engine
V_{T_V}	Tip speed for forward flight condition
w	Disc loading, lb/ft^2
W	Total aircraft weight for the condition under consideration
W_a	Engine air flow, lb/sec.
W_F	Fuel weight required
W_f	Fuel flow rate, lb/hr.
W_G	Gross weight
Δ_t	Time required for a given portion of the mission
ΔW_F	Fuel weight required for a given portion of the mission
z/D	Height of teeter point from the ground in rotor diameters
α	Blade section angle of attack
γ_e	Rotor radius to mean engine location radius (1.0)
δ_{o_B}	Blade coefficient of drag at and $\phi = 0$
δ_{2_B}	Coefficient of drag for use with $C_{L_{r_o}}^2$ in determining drag polar
δ_{o_I}	Nacelle coefficient of drag at and $\phi = 0$ based on compressor inlet area
δ_{2_I}	Coefficient of drag for use with compressor inlet area and $C_{L_{r_o}}^2$ in determining drag polar

δ'_{2I}	Coefficient of drag for use with compressor inlet area and ϕ^2
ξ	Ratio of blade radius to rotor radius (.981)
η	Overall efficient factor
ρ	Air mass density at altitude, slugs/ft^3
ρ_o	Air mass density at sea level
σ	Solidity $(A_b/\xi\pi R^2)$
ϕ	Nacelle yaw angle, radians

<u>Formula Summary</u>

$$C_{L_{r_o}} = \frac{.833 \times 10^6 W_G n^2}{B^3 V_{T_H}^{\,6}\,\sigma}$$

$$ihp_V = \frac{1.13(W)\,\frac{1}{B}\sqrt{\frac{W}{2\rho}}\,(K_u)}{550} \qquad \text{for } V = 0,\ K_u = 1$$

where $1.13 = ihp_\Delta/ihp_\Box$

$$K_u = \sqrt{\frac{1}{2}\left[\sqrt{\left(\frac{V}{u_H}\right)^4 + 4} - \left(\frac{V}{u_H}\right)^2\right]}$$

$$K_{\mu_b} = 1 + 3(V/\xi V_{T_V})^2 + 30(V/\xi V_{T_V})^4$$

$$K_{\mu_N} = 1 + (V/r_e V_{T_V})^2\left[1 + \frac{1}{2\delta_{m_I}}(\delta'_{2I} + a'_I)\right] + \frac{\delta_{2I}'}{2\delta_{m_I}}\left(\frac{V}{r_e V_{T_V}}\right)^4$$

$$Rhp_V = .2164 \times 10^{-5} V_{T_V}^{\,3}(\rho/\rho_o)\left[(A_b/4)\xi^3\delta_m B_o K_{\mu_B} + A_I \delta_{m_I} n_e^3 K_{\mu_N}\right]$$

$$\delta_m = \delta_o + \delta_2\, C_{L_{r_o}}^{\,2}\,(\rho_o/\rho)^2$$

PERFORMANCE SUMMARY

Item	Gross Weight (Lb.)			
	47,680	72,104	90,100	103,000
Max. speed at S.L. - V_T = 592 f.p.s. (knots)	133 (A_π = 200) 146 (A_π = 100)	127	123	-
Cruising speed at S.L. - V_T = 592 f.p.s. (knots)	93	100	105	111
Max. rate of climb at S.L. (ft/min.)	6,040	3,010	1,950	-
Vert. rate of climb at S.L. (ft/min.)	5,900	2,910	1,140	-
Hover ceiling out-of-ground effect - OAT = 95°F. (ft.)	-	6,060	-	-
Hover ceiling out-of-ground effect - standard day (ft.)	26,200	14,100	5,750	750
Service ceiling (ft.)	32,000	22,000	15,800	-

Note: All performance data for MRP.

A_π = 200 ft^2 and standard conditions except as noted. V_T = 650 f.p.s. except as noted.

1.0 INTRODUCTION

This report presents the aerodynamic characteristics and performance analysis of the proposed Hiller Aircraft Company's Model 1108 tip turbo-jet-powered heavy-lift rotor system.

This report also summarizes results of the parametric study of the design variables and their effects upon power requirements, performance characteristics, and rotor limitations.

Standard helicopter performance analysis methods (modified where required to account for tip propulsion) are used throughout, and all governing equations and curves accompanied by the appropriate references are included in the report.

2.0 DIMENSIONS AND CHARACTERISTICS

2.1 General

Number of engines	8
Number of blades	4
Design gross weight	72,104 lb.
Empty weight	34,700 lb.

Equivalent flat plate (C_D = 1.0) drag area, A_π

a) Outbound (with external payload)	200 sq. ft.
b) Inbound (without external payload)	100 sq. ft.

(Crane-type fuselage)

2.2 Rotor Characteristics

Main rotor:

Rotor type	Spring restrained, teetering, universal
Rotor diameter, ft. (Engine ℄ to engine ℄).................	111.8
Blade twist, deg.	-10^{o}
Blade chord (constant), ft.	6.5
Blade airfoil section (constant)	0015
Blade area, sq. ft.	1,426
Disk area, sq. ft.	9,817
Solidity	.148
Tip speed, f.p.s.	
a) Hover	650
b) Cruise	592
Design mean blade lift coefficient, $C_{L_{r_o}}$	3296
Design disk loading, lb/ft^2	7.3
Blade aspect ratio	8.6

2.3 Airfoil Dimensional Properties and Ordinates

Listed on the following page are the true airfoil ordinates, based on a 6.5-foot (78-inch) constant chord, for the NACA 0015 airfoil selected for the Model 1108.

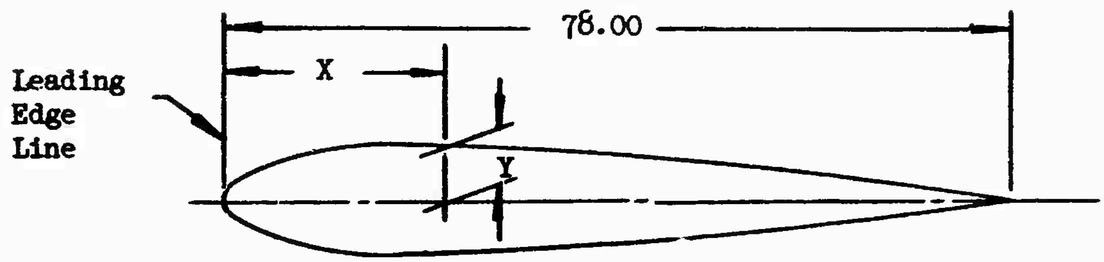

Chord Station (%)	X (In.)	Y (In.)
0	0	0
1.25	.875	1.846
2.50	1.950	2.549
5.00	3.900	3.466
7.50	5.850	4.095
10.00	7.800	4.565
15.00	11.700	5.212
20.00	15.600	5.594
25.00	19.500	5.793
30.00	23.400	5.658
40.00	31.200	5.658
50.00	39.000	5.161
60.00	46.800	4.449
70.00	54.600	3.572
80.00	62.400	2.558
90.00	70.200	1.412
95.00	74.100	.786
100.00	78.00	0

Leading edge radius = 2.48 in.

2.4 Aircraft Group Weight Statement

Rotor group		16,398 lb.
Blades	15,561	
Hub	837	
Pylon group		1,731
Tail group		473
Tail rotor	216	
Stabilizer	257	
Body group		3,203
Landing gear group		2,897
Flight controls group		1,434
Engine section group		1,359
Propulsion group		5,539
Engines (357-1)	2,920	
Cooling system	80	
Gearboxes and drives	367	
A.P.U. units	365	
Starting system	140	
Engine controls	100	
Fuel system	1,292	
Rotor mast	275	
Instrument group		296
Electrical group		750
Electronics group		275
Furnishings group		345
		34,700 lb.

Empty weight	34,700 lb.
Crew	400
Oil	80
Cargo	24,000
Fuel	12,924
Gross weight	72,104 lb.

2.5 Power Plant System

2.5.1 Engine

Power is provided by eight Continental Model 357-1 turbojet engines; i.e., two engines mounted at the tip of each of four blades. The static sea-level performance targets for the fully qualified production model are summarized below.

Military rated power	**1,700 lb. - 0.99 SFC**
Normal rated power	**1,375 lb. - 0.98 SFC**

Of particular interest are the estimated performance curves supplied this company by the engine manufacturer, herein included as Figures 1 through 4.

2.5.2 Fuel System

The tentative fuel system consists of two identical, independent, but interconnected fuel systems feeding fuel to two stacked manifolds located at the rotor hub. The upper manifold will service the upper engine on each of the four blades; the lower manifold will service the lower engines on the rotor blades. The fuel is transferred from the rotor hub to the engine fuel controls by centrifugal force.

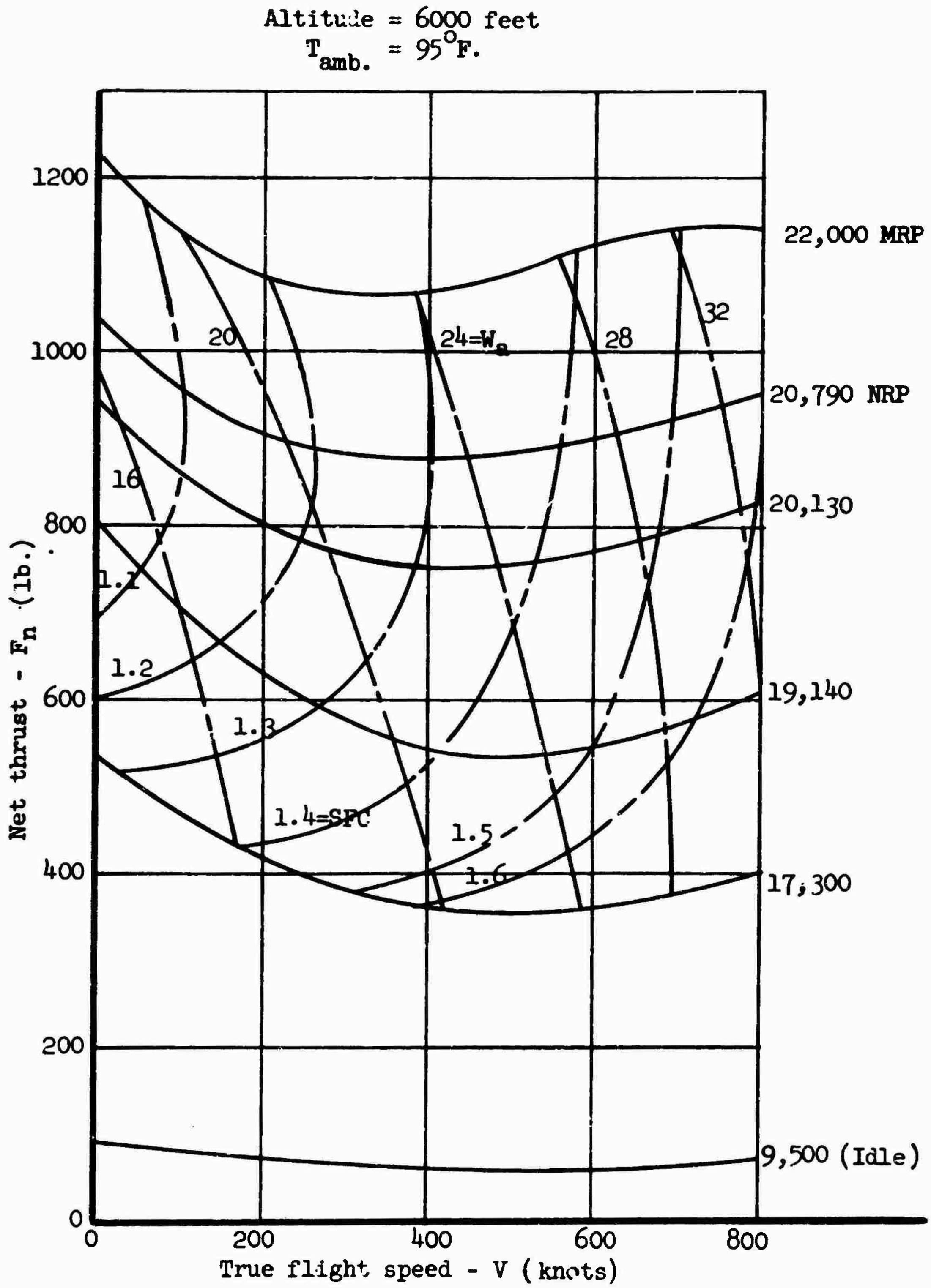

Figure 1. 357-1 Estimated Performance - Net Thrust Versus Flight Speed.

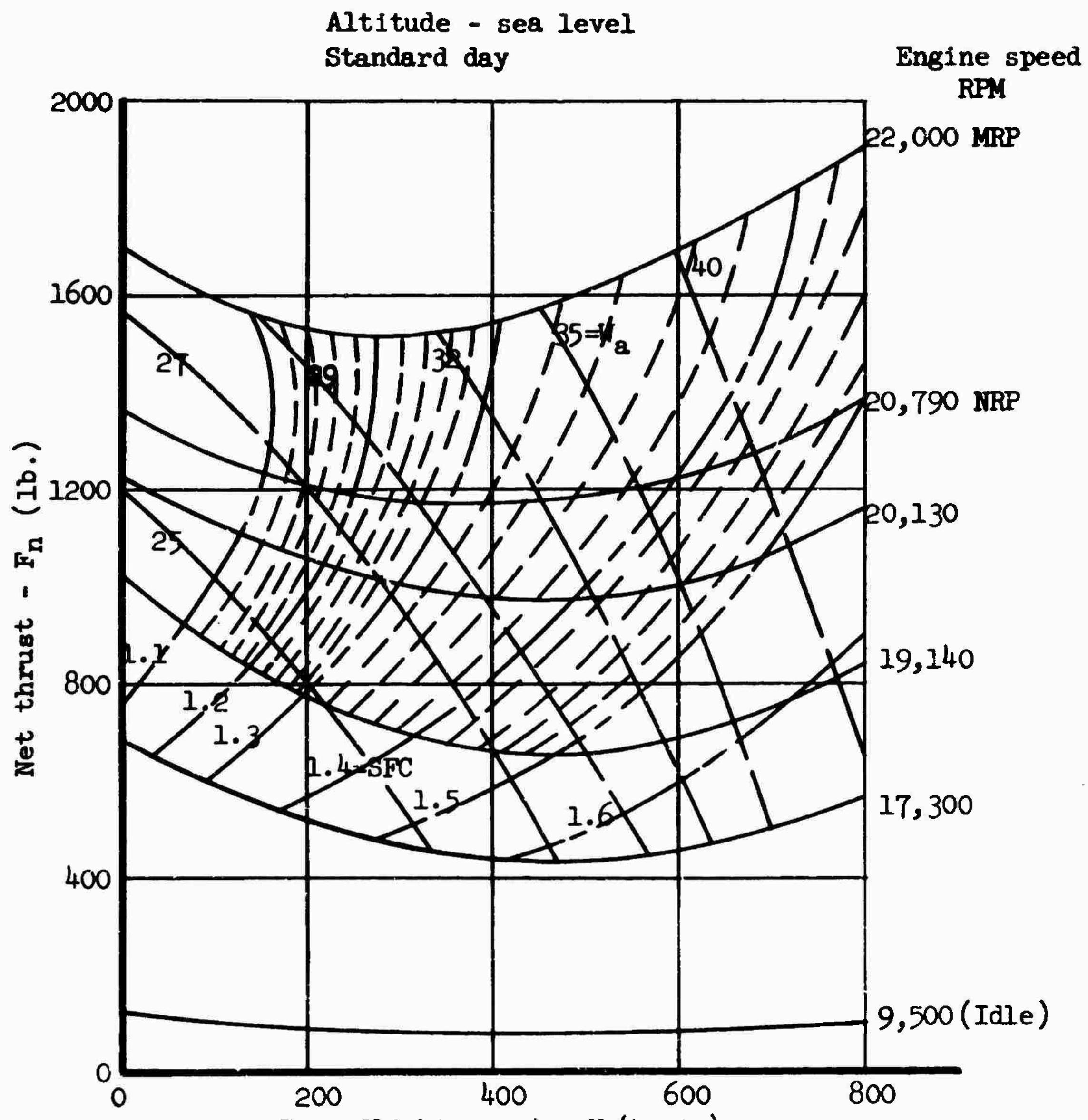

Figure 2. 357-1 Estimated Performance - Net Thrust Versus Flight Speed.

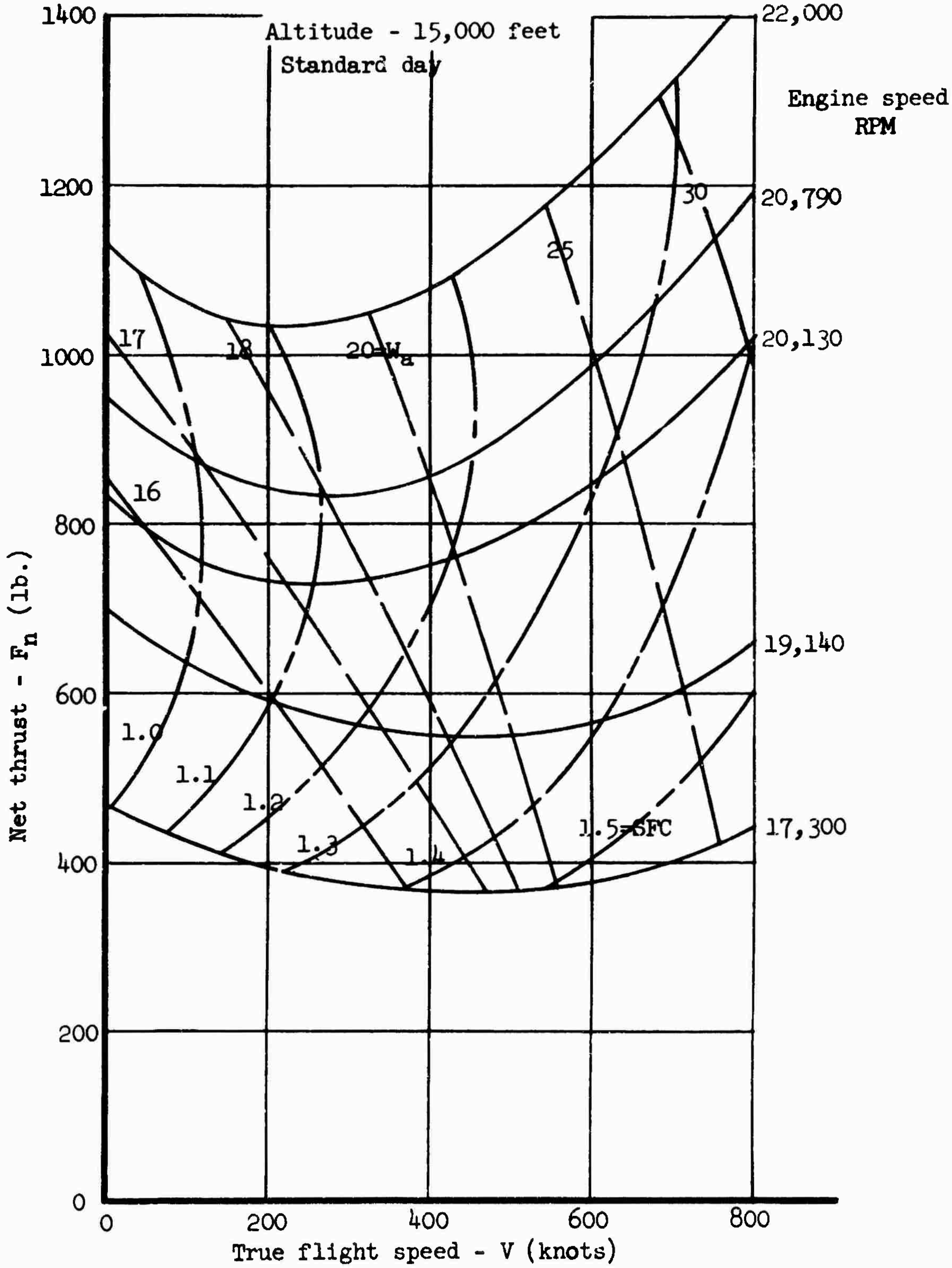

Figure 3. 357-1 Estimated Performance - Net Thrust Versus Flight Speed.

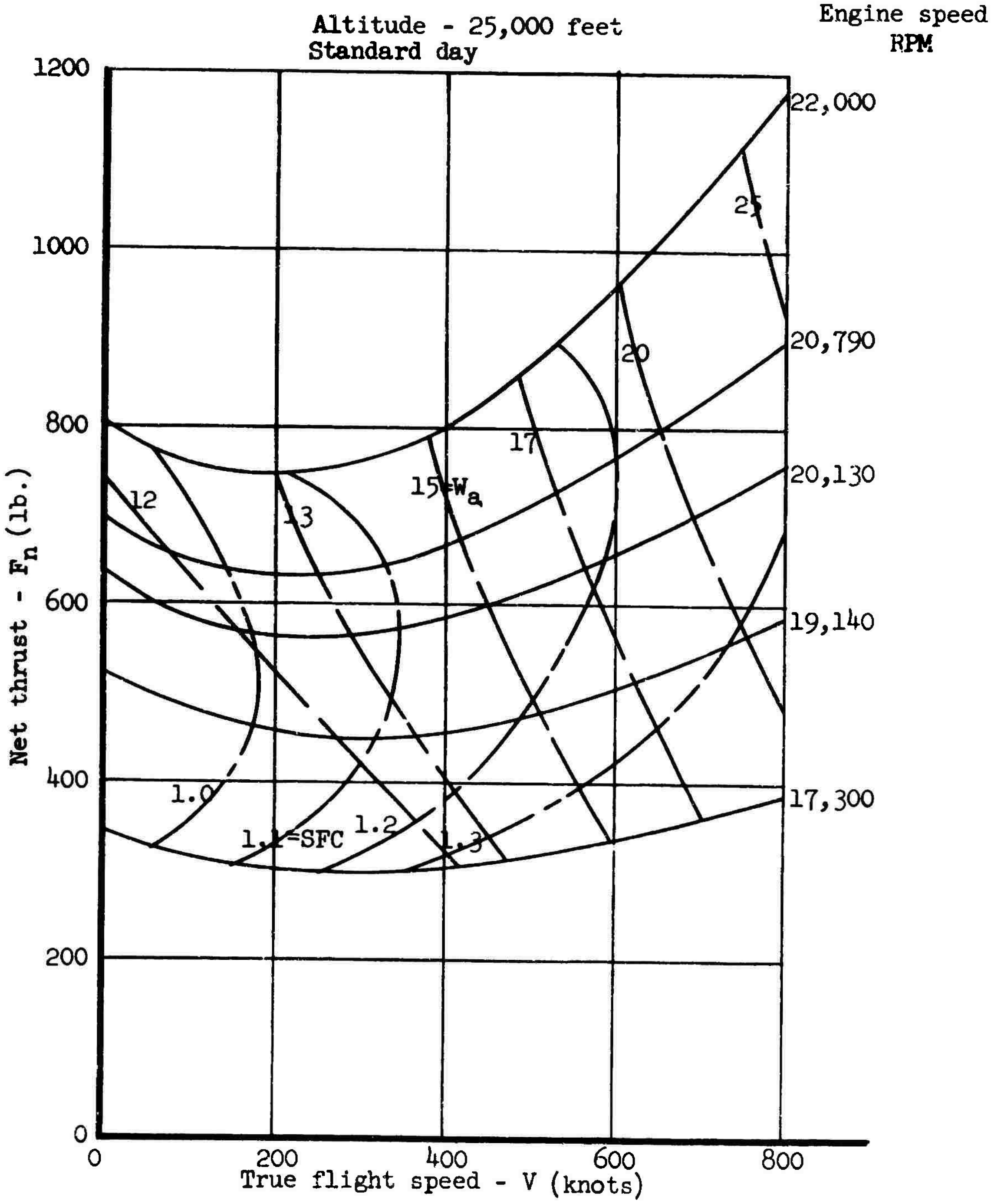

Figure 4. 357-1 Estimated Performance - Net Thrust Versus Flight Speed.

3.0 AERODYNAMIC DATA

3.1 Rotor Blade Section Characteristics

The 0015 airfoil is selected for the Model 1108 primarily for its section properties. That is, a relatively thick blade is needed to provide adequate space for service lines which must be installed within the blade and its deep section is required to provide sound structural media to which the tip-mounted engines may be fixed.

3.2 Rotor Parameters

The selection of rotor parameters was based on meeting the performance requirements as outlined in Reference 2. To obtain the many combinations of rotor parameters which would satisfy the above requirements, a parametric study was conducted in which the major variables were gross weight (W_G), disk loading (w), main rotor tip speed (V_T), and design mean blade lift coefficient ($C_{L_{r_o}}$). The aerodynamic equations were then developed in terms of these variables. For selected values of V_T and $C_{L_{r_o}}$, the solution of simultaneous equations yielded values for W_G and w which satisfy the performance requirement under investigation.

A comprehensive discussion of the approach, methods used, and the final selection of design parameters through a series of limiting cutoffs (aerodynamic, weight, size, and structural) will be found in the Tip Turbojet Parametric Design Study, Volume II.

3.3 Equivalent Flat Plate Area

For the purpose of the parametric and performance studies, the total fuselage (plus cargo) equivalent flat-plate area (based on $C_D = 1.0$) has been established as follows:

Outbound (external payload) - $A_\pi = 200 \text{ ft}^2$

Inbound (no external payload)- $A_\pi = 100 \text{ ft}^2$

These values merely reflect the anticipated equivalent flat plate areas.

4.0 POWER REQUIRED

Power requirements for level flight are obtained from the summation of the rotor induced power, rotor profile-drag power, fuselage parasite power, mechanical gear losses, and miscellaneous power required to operate hydraulic and electrical equipment. Standard helicopter performance analysis methods, as outlined in Reference 3, were modified to include tip-powered helicopters.

Complete derivations for the induced and profile power equations may be found in Volume II, Parametric Study.

4.1 Induced Power

From momentum considerations the thrust of a hovering rotor may be expressed by

$$T = \rho A u_H (\Delta v) \tag{1}$$

Conventional propeller theory establishes the relationship between the increase in velocity of the air above the rotor and the increase which occurs behind the rotor; namely

$$\Delta u_{above} = \Delta u_{below}$$

or

$$\Delta v = 2u_H$$

Therefore, the thrust of a hovering rotor is

$$T = \rho A u_H (2u_H) = 2\rho\pi R^2 u_H^2 \tag{2}$$

from which the induced velocity, u_H, through the rotor is

$$u_H = \frac{T}{2\rho\pi R^2} = \frac{w}{2\rho} \tag{3}$$

The term $w = T/\pi R^2$ is the rotor disk loading.

At this point a tip loss factor B is introduced to allow for the reduction in rotor thrust at the blade tip (finite aspect-ratio blade). For preliminary work, a constant value of B = .964 for the main rotor is considered representative and is consistent with the NACA empirical solution given by the expression

$$B = 1 - \frac{\sqrt{2C_T}}{b}$$

where b = number of blades

C_T = thrust coefficient = $T/\pi R^2 \rho V_T^2$

Substituting $(BR)^2$ for $(R)^2$ in Equation (3) establishes the hovering induced velocity, considering blade tip losses, as

$$u_H = \frac{1}{B}\sqrt{\frac{W}{2\rho}} \tag{4}$$

Equation (4) assumed that the spanwise inflow distribution is uniform (theoretical). In actuality, the distribution is more nearly triangular which, as shown in Appendix A, Part I, of Reference 4, increases the induced horsepower by a factor of 1.13. That is

$$\frac{ihp_{\Delta}}{ihp_{\square}} = 1.13 \tag{5}$$

Rewriting Equation (4) to include this modification of the inflow distribution yields:

$$u_H = \frac{1.13}{B}\sqrt{\frac{W}{2\rho}} \tag{6}$$

Substitution of the 1.13 factor is based upon hovering inflow velocity surveys and measured main rotor flight vibratory loads on the H-23 series helicopters.

The variation of induced velocity, u, with forward velocity is now introduced by defining the induced velocity factor K_u where

$$K_u = u_i/u_H \tag{7}$$

Therefore, substituting Equation (7) in Equation (6) and solving for u_i

$$u_i = \frac{1.13}{B}\sqrt{\frac{W}{2\rho}}\,(K_u) \tag{8}$$

The derivation of K_u is presented in Appendix A, Reference 4. For convenience in calculating induced velocity, a plot of K_u as a $f(V/u_H)$ is presented in Figure 5.

From work-energy considerations, the induced horsepower required to produce thrust is:

$$ihp = \frac{Tu_i}{550} = \frac{(W)\,\frac{1.13}{B}\sqrt{\frac{W}{2\rho}}\,(K_u)}{550} \tag{9}$$

Inasmuch as rotor tilt angles are to or less than 10 degrees, small angle assumptions are valid. Therefore, T = W.

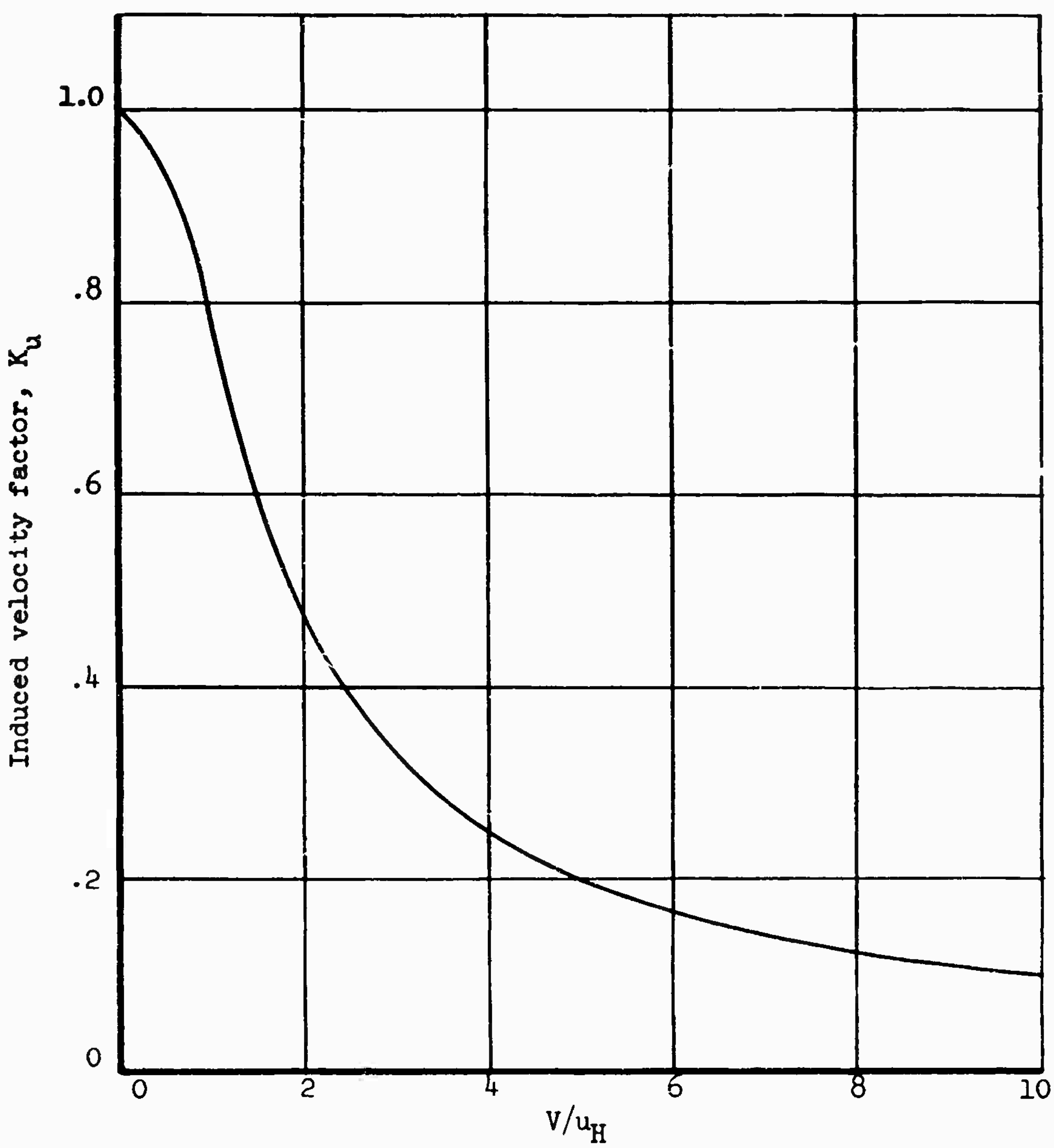

Figure 5. Induced Velocity Factor, K_u, as a Function of Forward Velocity.

Sample Calculation: Hover, OGE, S.L. 71,680 pounds, standard day.

$w = 7.3\ \mathrm{lb/ft^2}$ (Section 2.2)

$K_u = 1.00$ (Figure 1)

$$\mathrm{ihp} = \frac{1.13(71{,}680)\left[\frac{1}{.964}\sqrt{\frac{7.3}{2(.002378)}}\right](1.00)}{550} = 5{,}985\ \mathrm{hp}$$

4.2 Profile Power

As derived in the parametric design study, the profile power of the main rotor may be expressed by the equation

$$\mathrm{Rhp}_V = .2164 \times 10^{-5} V_T^3 \left[\left(\frac{A_b}{4}\, \xi^3 \delta_{m_{B_o}} K_{\mu_b}\right) + (A_I \delta_{m_I} \Upsilon_e^3 K_{\mu_N})\right]\frac{\rho}{\rho_o} \qquad (10)$$

where:

V_T = tip speed in hover = 650 f.p.s. (Section 2.2)

A_b = effective blade area = 1,426 ft^2 (Section 2.2)

ξ = rotor blade to rotor radius correction = .981

$\delta_{m_B} = \delta_{o_B} + \delta_{2_B}\, C_{L_{r_o}}^2 (\rho_o/\rho)^2$ = mean blade drag coefficient

$= .009 + .00927\, C_{L_{r_o}}^2 (\rho_o/\rho)^2$

$$K_{\mu_b} = 1 + 3(V/\xi V_T)^2 + 30(V/\xi V_T)^4 \qquad (11)$$

A_I = total compressor inlet area = 8.48 ft^2

$\delta_{m_I} = \delta_{o_I} + \delta_{2_I} C_{L_{r_o}}^2 (\rho_o/\rho)^2$ = mean nacelle drag coefficient

$= .282 + .100\, C_{L_{r_o}}^2 (\rho_o/\rho)^2$

Υ_e = ratio of rotor radius to mean engine location radius

$= 1.00$

$$K_{\mu_N} = 1 + (V/\Upsilon_e/V_T)^2\left[1 + \frac{1}{2\delta_{m_I}}(\delta'_{2_I} + a'_I)\right] + \frac{\delta'_{2_I}}{2\delta_{m_I}}\left(\frac{V}{\Upsilon_e V_T}\right)^4 \qquad (12)$$

The constants, as contained in the forward velocity terms (profile power factors K_{μ_b} and K_{μ_N}), and determined in the parametric study, Reference 7, are as follows:

$$\delta'_{2_I} = 5.0$$

$$a'_I = 4.5$$

Substituting the main rotor parameters into Equations (10), (11), and (12) yields

$$Rhp_V = (200{,}021.04\delta_{m_B}K_{\mu_b} + 5{,}039.57\delta_{m_I}K_{\mu_N})\rho/\rho_o \tag{13}$$

$$K_{\mu_b} = 1 + 3(V/637.65)^2 + 30(V/637.65)^4 \tag{14}$$

$$K_{\mu_N} = 1 + (V/650)^2\left(1 + \frac{9.5}{2\delta_{m_I}}\right) + \frac{5.0}{2\delta_{m_I}}(V/650)^4 \tag{15}$$

Sample Calculation: Hover, OGE, S.L., 71,680 pounds, standard day.

$$K_{\mu_b} = 1.0$$

$$K_{\mu_N} = 1.0$$

$$\delta_{m_B} = .009 + .00927(.3296)^2(1)^2 = .009 + .0009973 = .0099973 = .010$$

$$\delta_{m_I} = .282 + .100(.3296)^2(1)^2 = .282 + .0107584 = .2927584 = .293$$

then

$$Rhp_V = (200{,}021.04)(.010)(1) + (5{,}039.57)(.293)(1) = 2{,}000.2 + 1{,}476.6$$
$$= 3{,}477 \text{ hp}$$

4.3 Parasite Power

Parasite power is found from the standard relationship

$$php = \frac{DV}{550} \tag{16}$$

where the drag, D, is given by the equation

$$D = 1/2\rho V^2 S C_D \tag{17}$$

Expressing the drag in terms of equivalent flat plate area, A_π (based on a drag coefficient, $C_D = 1.00$)

$$D = 1/2\rho V^2 A_\pi \tag{18}$$

Equation (16) may be rewritten in the form

$$php = \left(\frac{\rho_o V^3 A_\pi}{1{,}100}\right)\frac{\rho}{\rho_o} \tag{19}$$

Sample calculation: V = 100 knots, S.L., outgoing, standard day.

$$\text{php} = \frac{.002378(100 \times 1.689)^3(200)}{1,100} = \frac{.002378 \times 10^6(4,819)(2)}{11}$$

$$= \frac{.02292 \times 10^6}{11} = .002084 \times 10^6 = 2,084 \text{ hp}$$

4.4 Miscellaneous Power Losses

Two additional sources of power loss must be considered; namely,

a) Mechanical losses exemplified by friction and power transmission resulting in a system efficiency of 99-1/2 percent.

b) Accessory power resulting out of the power requirements for

   1) Primary flight instruments
   2) Partial hydraulic system power estimated total (hp_{misc}) = 100 hp

4.5 Tail Rotor Power

The tail rotor power requirement is considered to be 2.5 percent of the main rotor power, constant with forward speed and altitude.

Since the tail rotor power and system efficiency can both be expressed as a percentage of main rotor power, they may be combined into an overall efficiency factor of $\eta = .97$.

Tail rotor power and the 100 miscellaneous horsepower are to be supplied by twin auxiliary power units taken to have a specific fuel consumption equal to the main engines.

4.6 Total Power Required

The total power required for equilibrium flight is the summation of the general power expressions derived in Sections 4.1 through 4.4.

$$\text{rhp} = \frac{1}{\eta}(\text{ihp} + \text{Rhp} + \text{php}) + \text{hp}_{misc} \tag{20}$$

Sample calculation: Hover, S.L., 71,680 pounds, OGE, standard day.

$1/\eta = 1/.97 = 1.031$

ihp = 5,985 hp (Section 4.1)

Rhp = 3,477 hp (Section 4.2)

$$php = 0 \text{ hp}$$

$$hp_{misc} = 100 \text{ hp (Section 4.4)}$$

$$rhp = 1.031(5{,}985 + 3{,}477) + 100 \quad \text{(Equation (20)}$$

$$= 9{,}855 \text{ hp}$$

Total power required calculations were performed on the Bendix G-15 Digital Computer, and the results, in the form of curves of power required versus forward velocity for various gross weights and altitudes, are presented in Figures 6 through 10a.

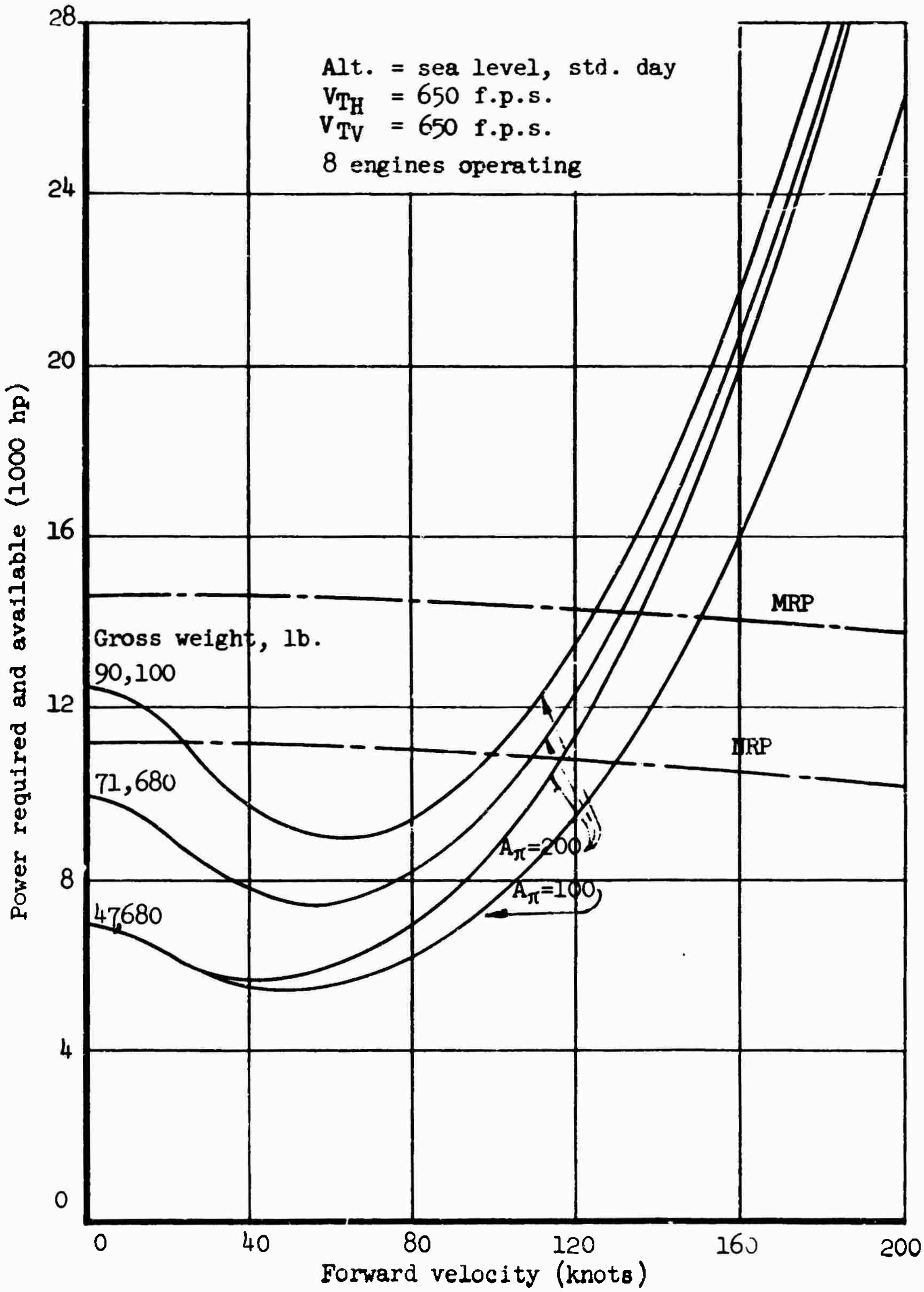

Figure 6. **Power Required and Power Available Versus Forward Velocity - Sea Level.**

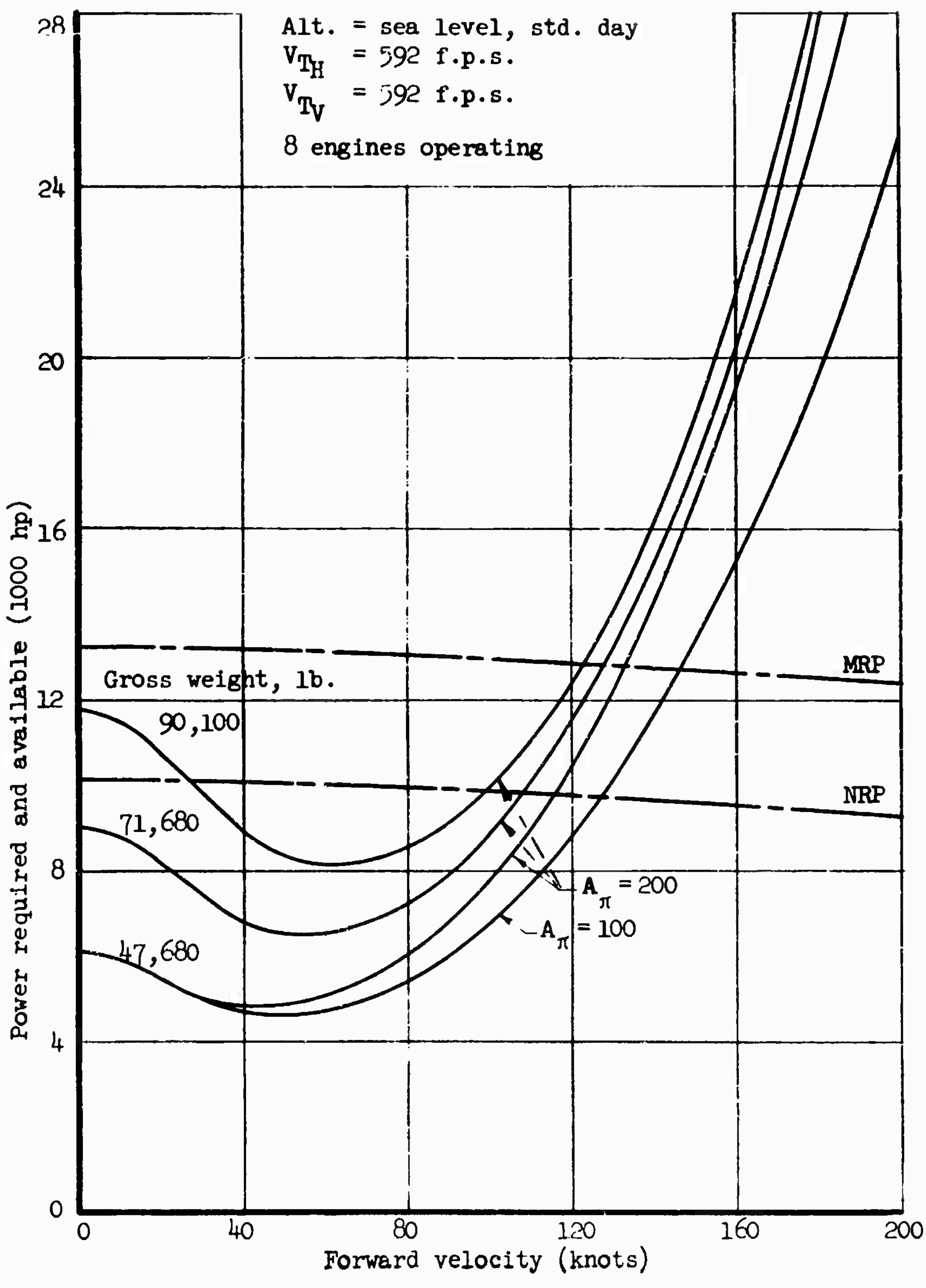

Figure 6a. Power Required and Power Available Versus Forward Velocity.

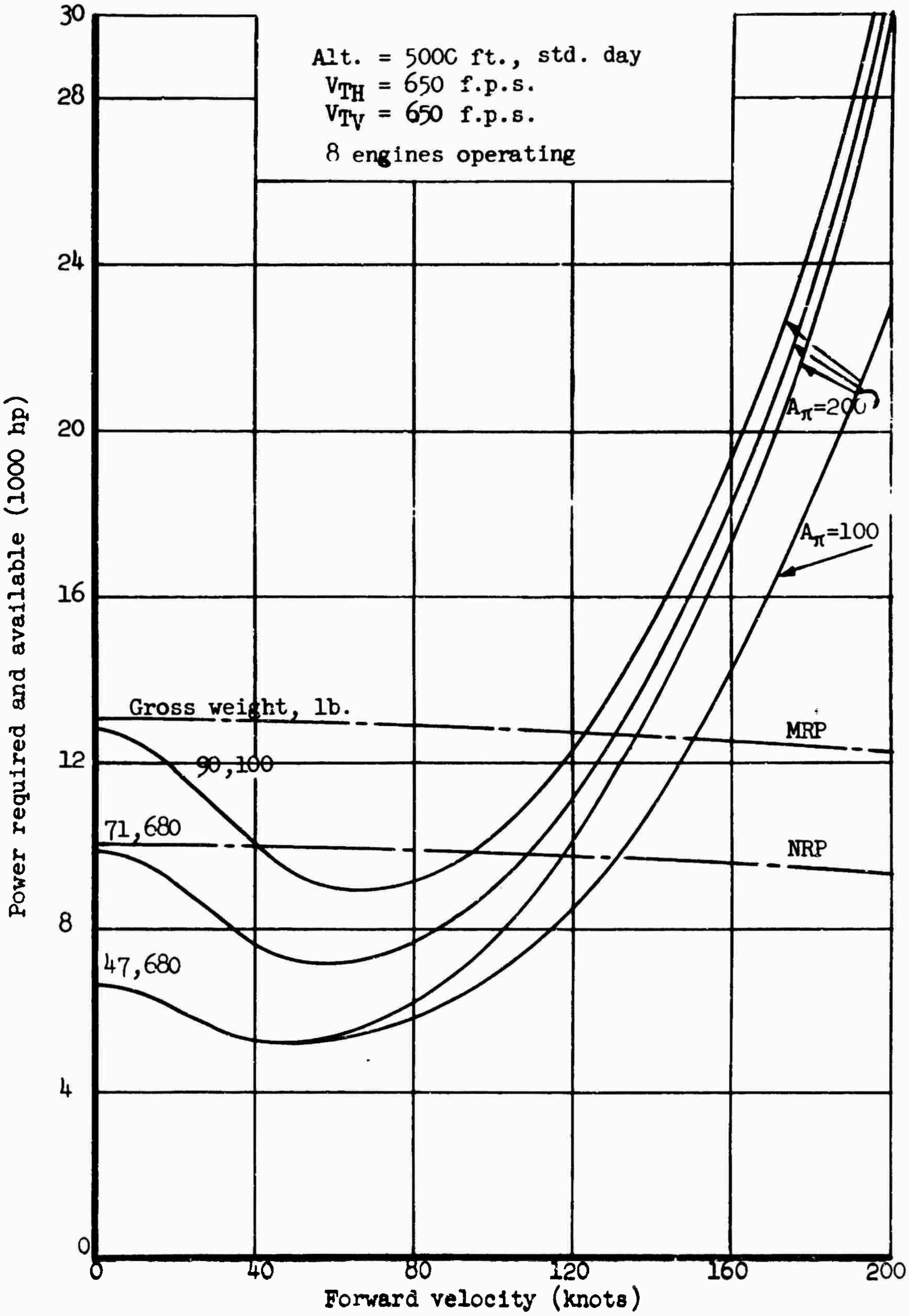

Figure 7. Power Required and Power Available Versus Forward Velocity - 5,000 Ft. Altitude.

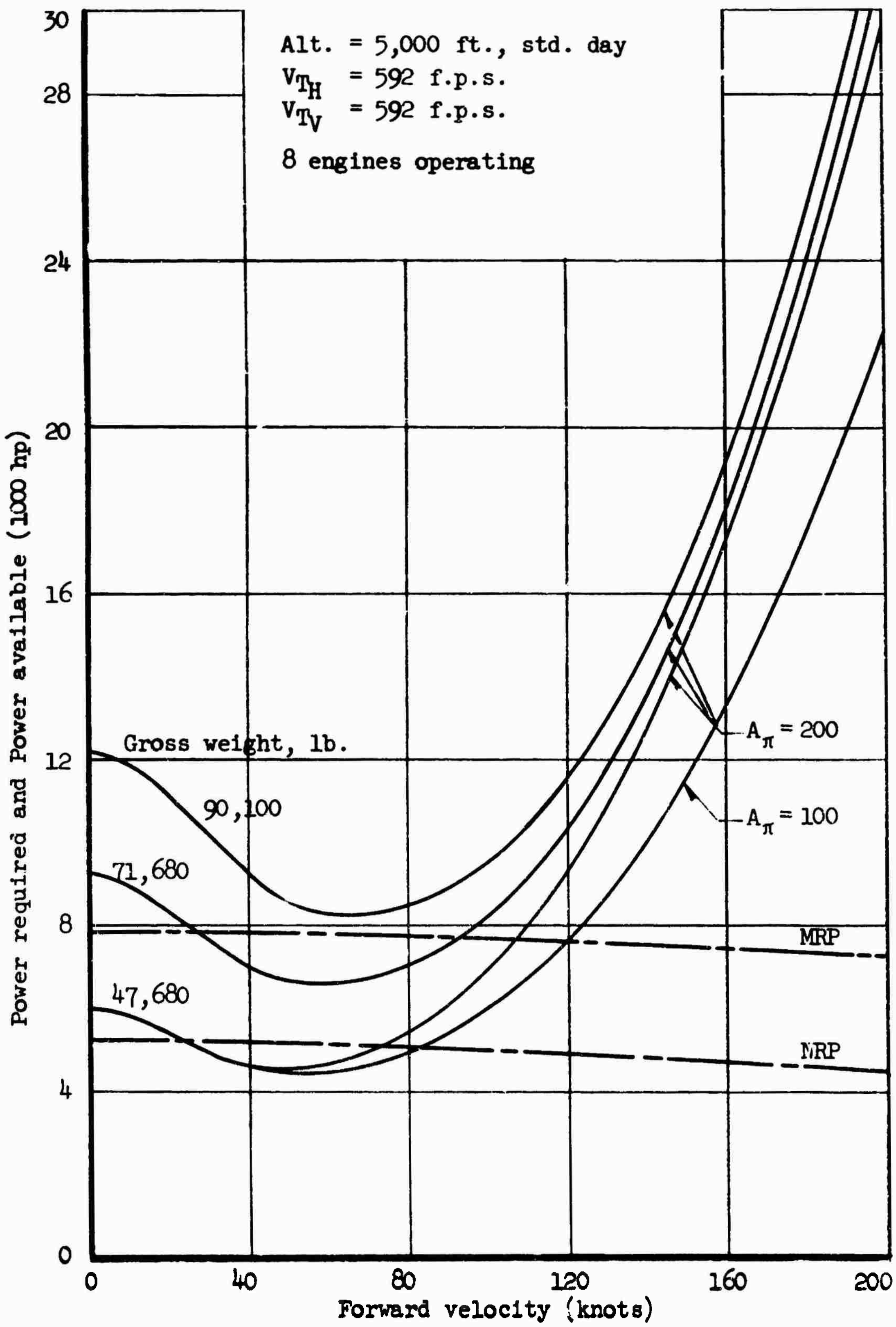

Figure 7a. Power Required and Power Available Versus Forward Velocity - 5,000 Ft. Altitude.

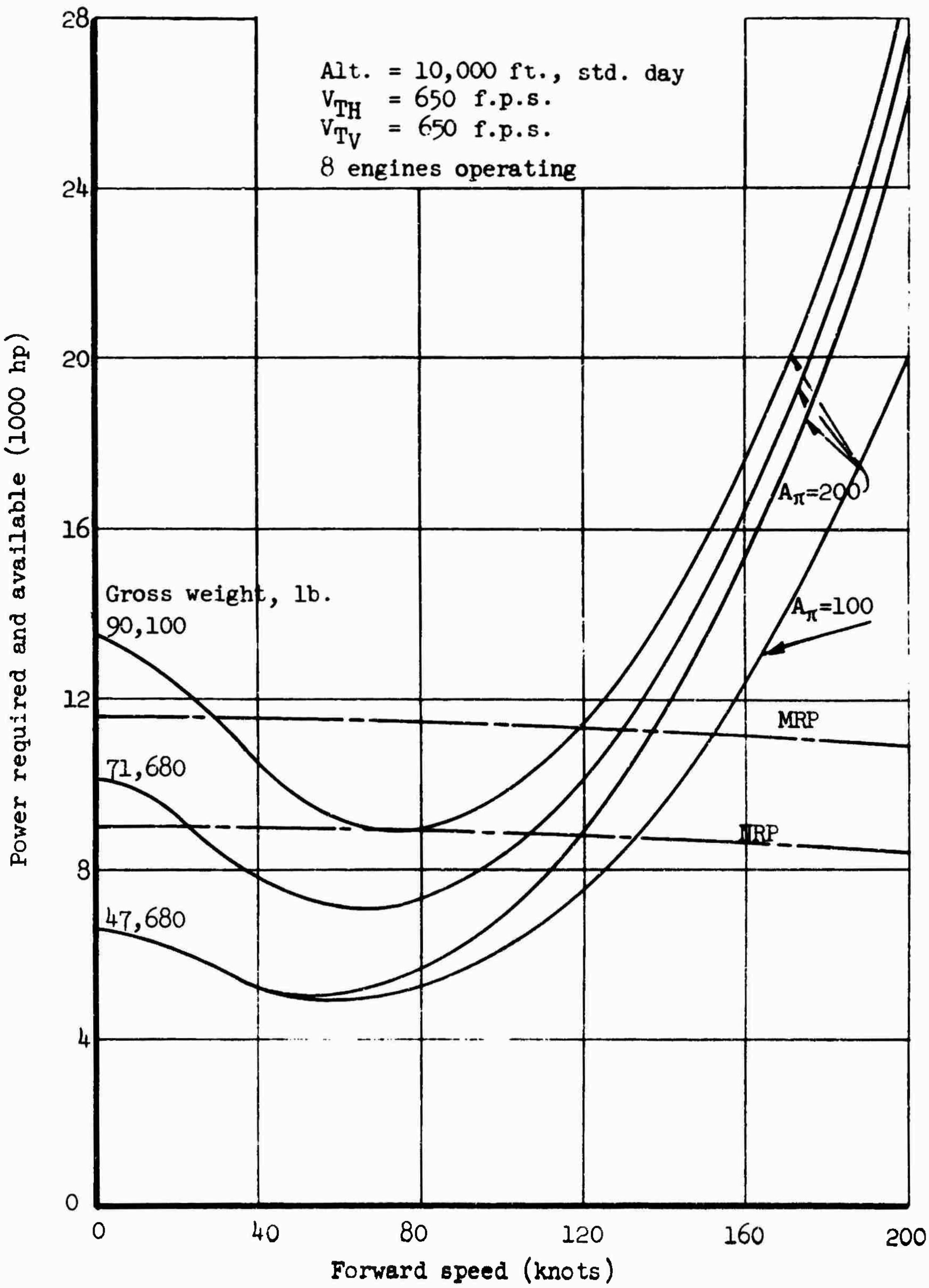

Figure 8. Power Required and Power Available Versus Forward Velocity - 10,000 Ft. Altitude.

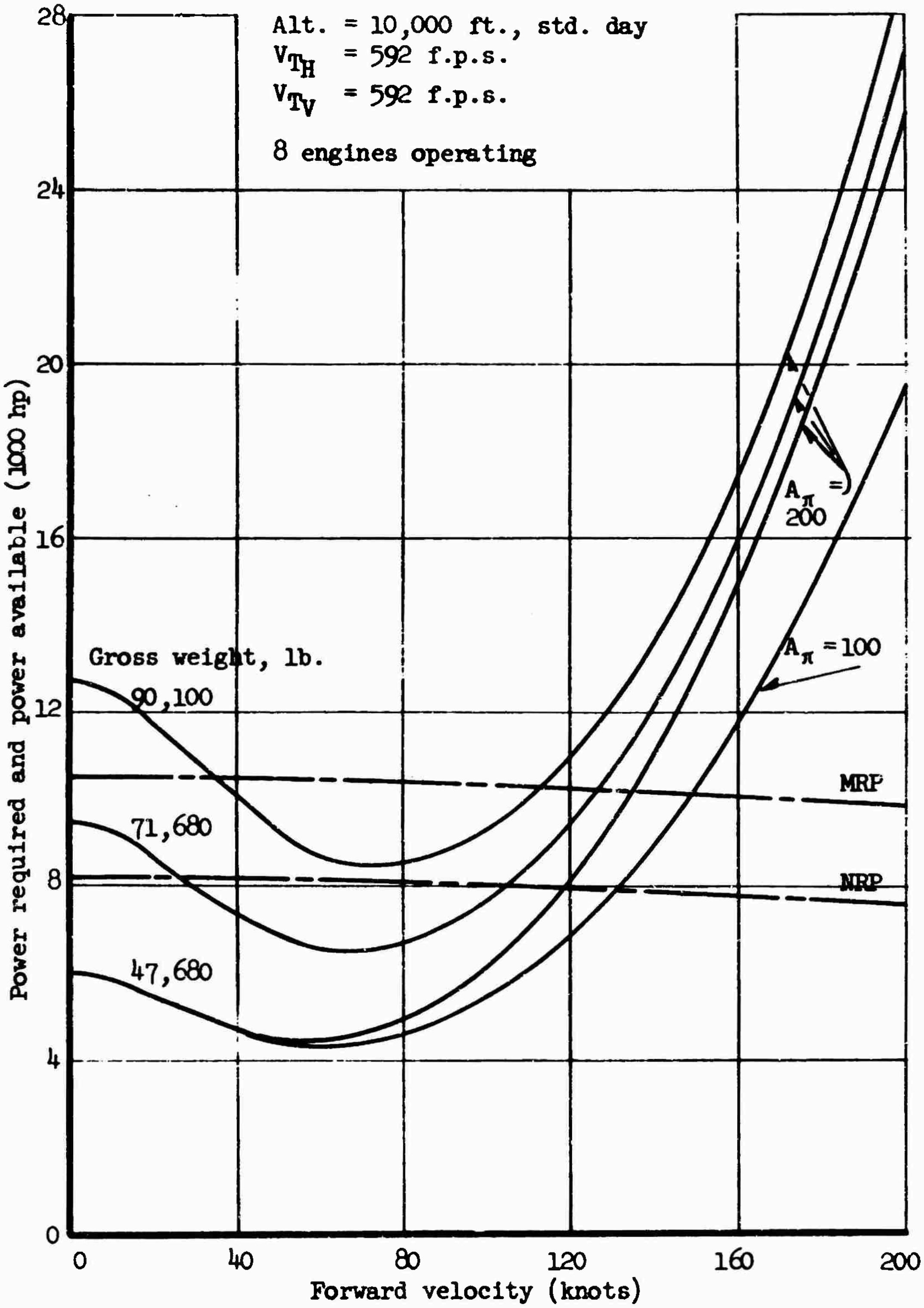

Figure 8a. **Power Required and Power Available Versus Forward Velocity - 10,000 Ft. Altitude.**

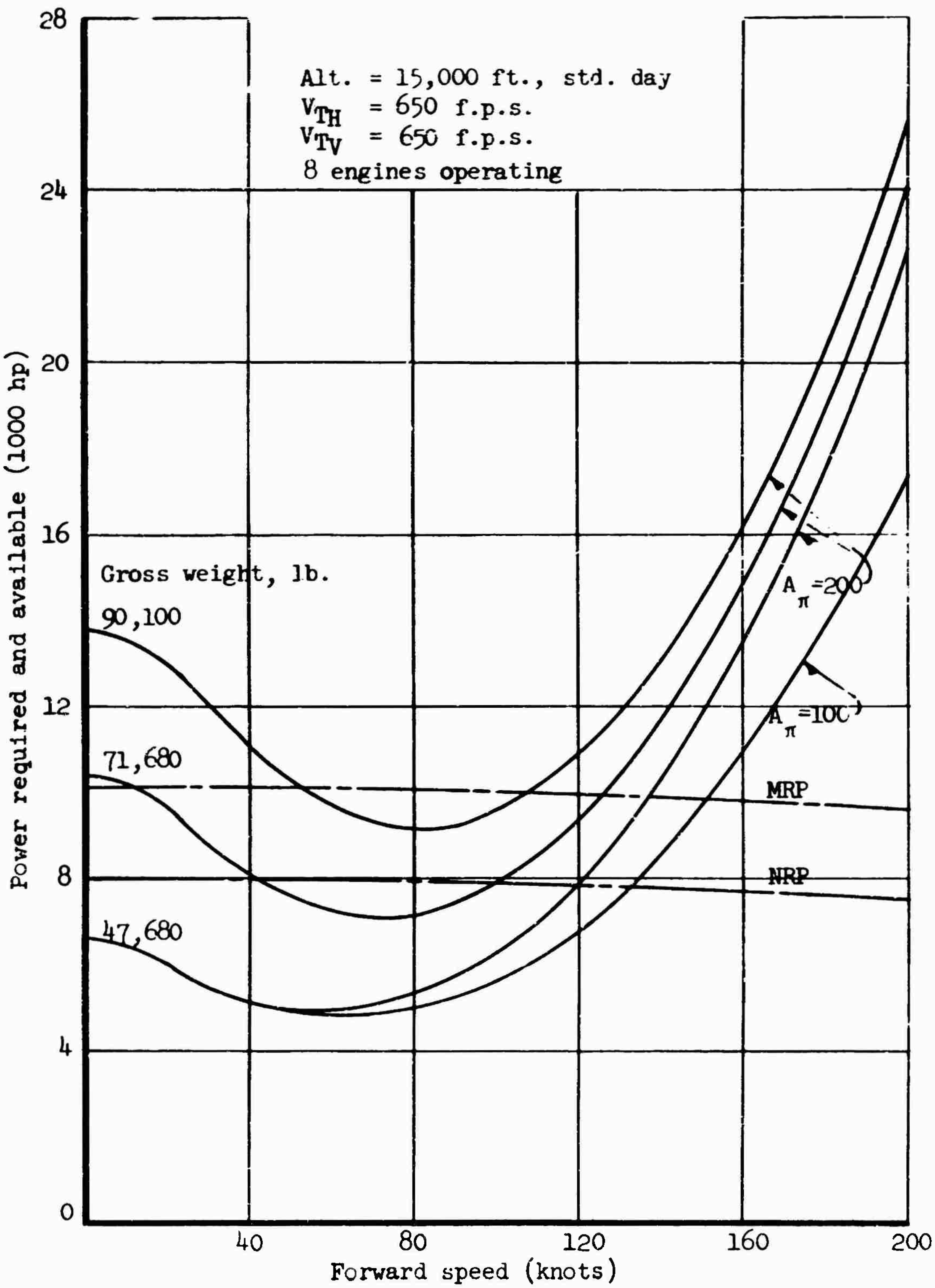

Figure 9. Power Required and Power Available Versus Forward Velocity - 15,000 Ft. Altitude.

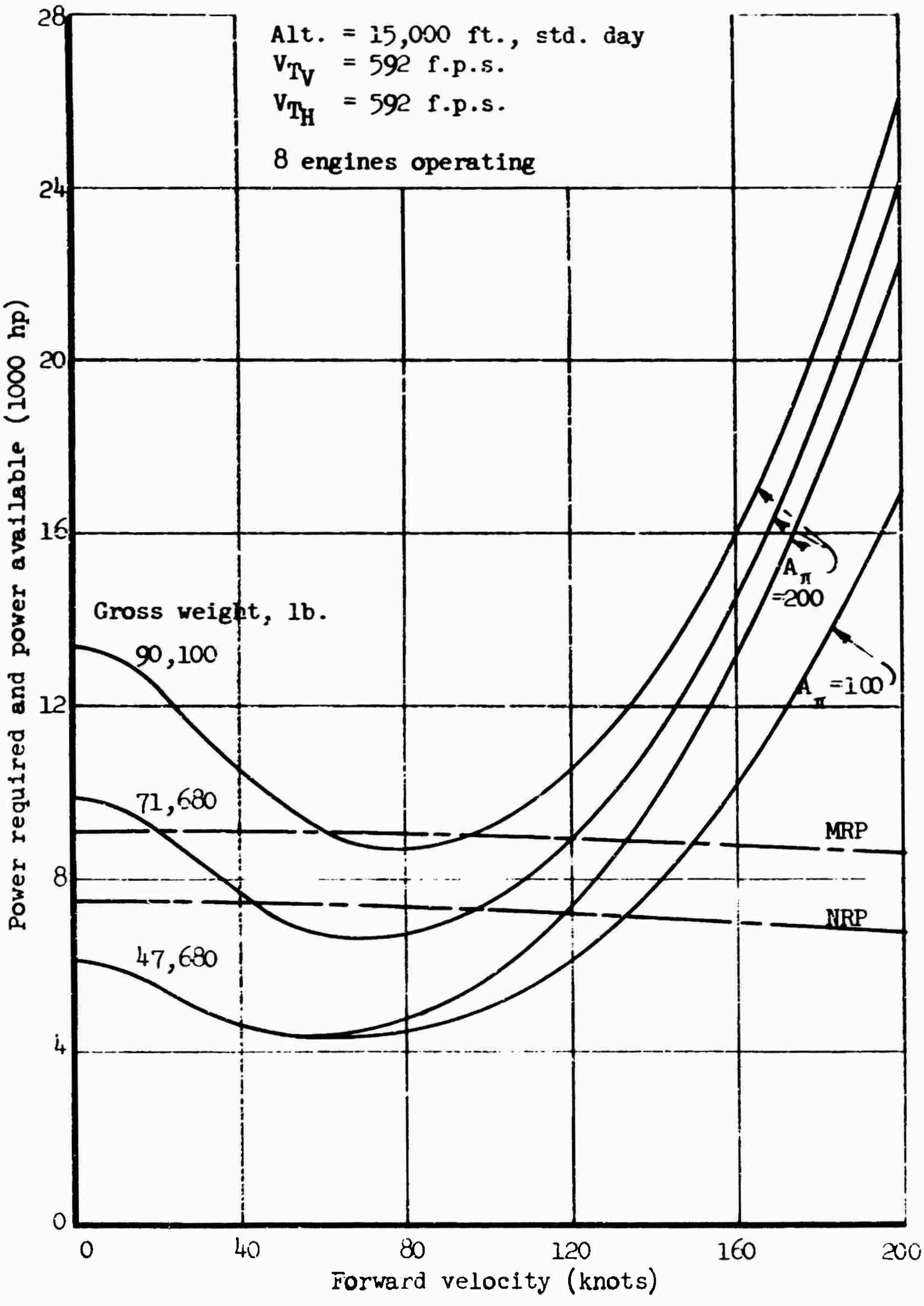

Figure 9a. Power Required and Power Available Versus Forward Velocity - 15,000 Ft. Altitude.

Alt. = 20,000 ft., std. day.
V_{T_H} = 650 f.p.s.
V_{T_V} = 650 f.p.s.

8 engines operating

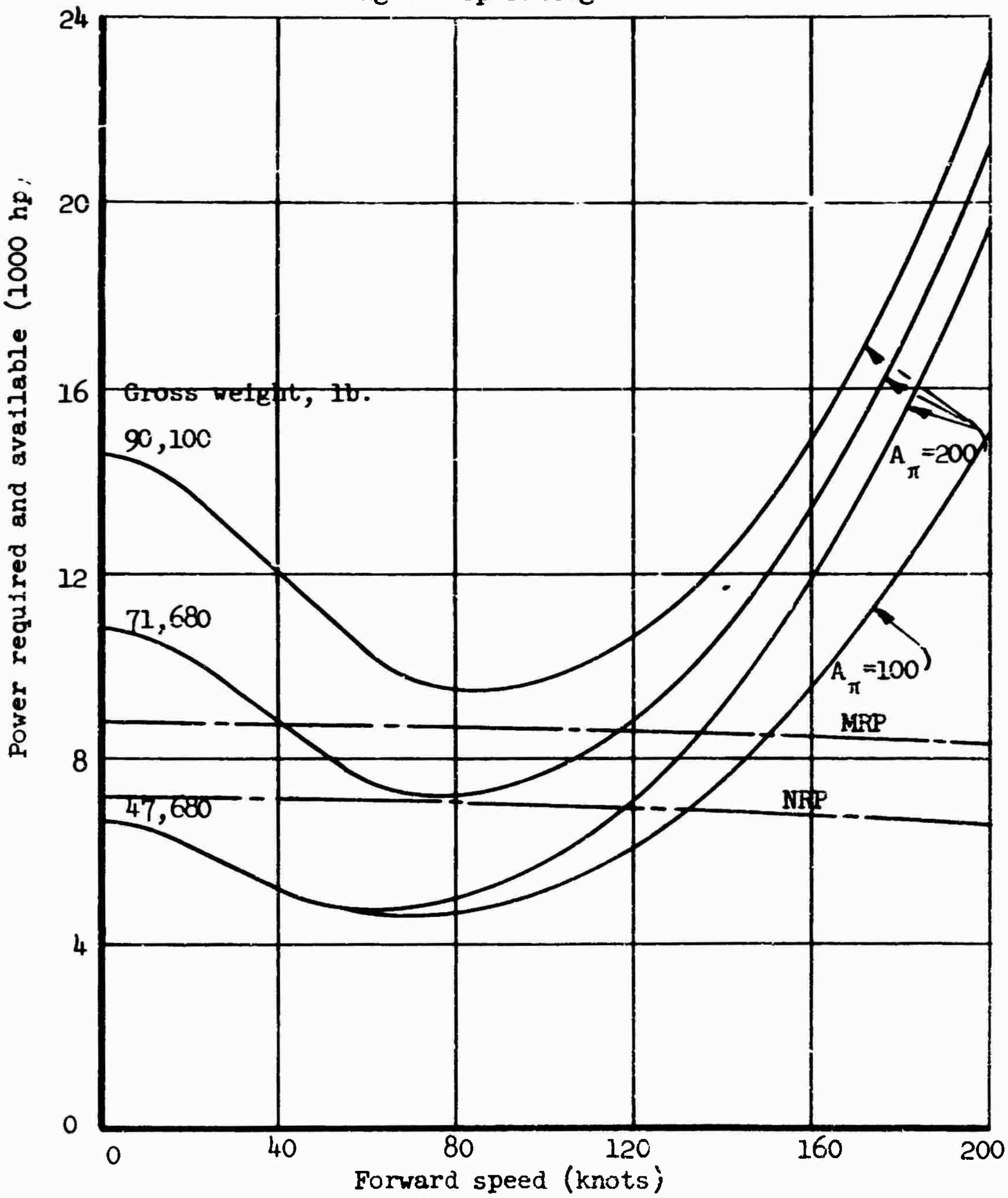

Figure 10. Power Required and Power Available Versus Forward Velocity - 20,000 Ft. Altitude.

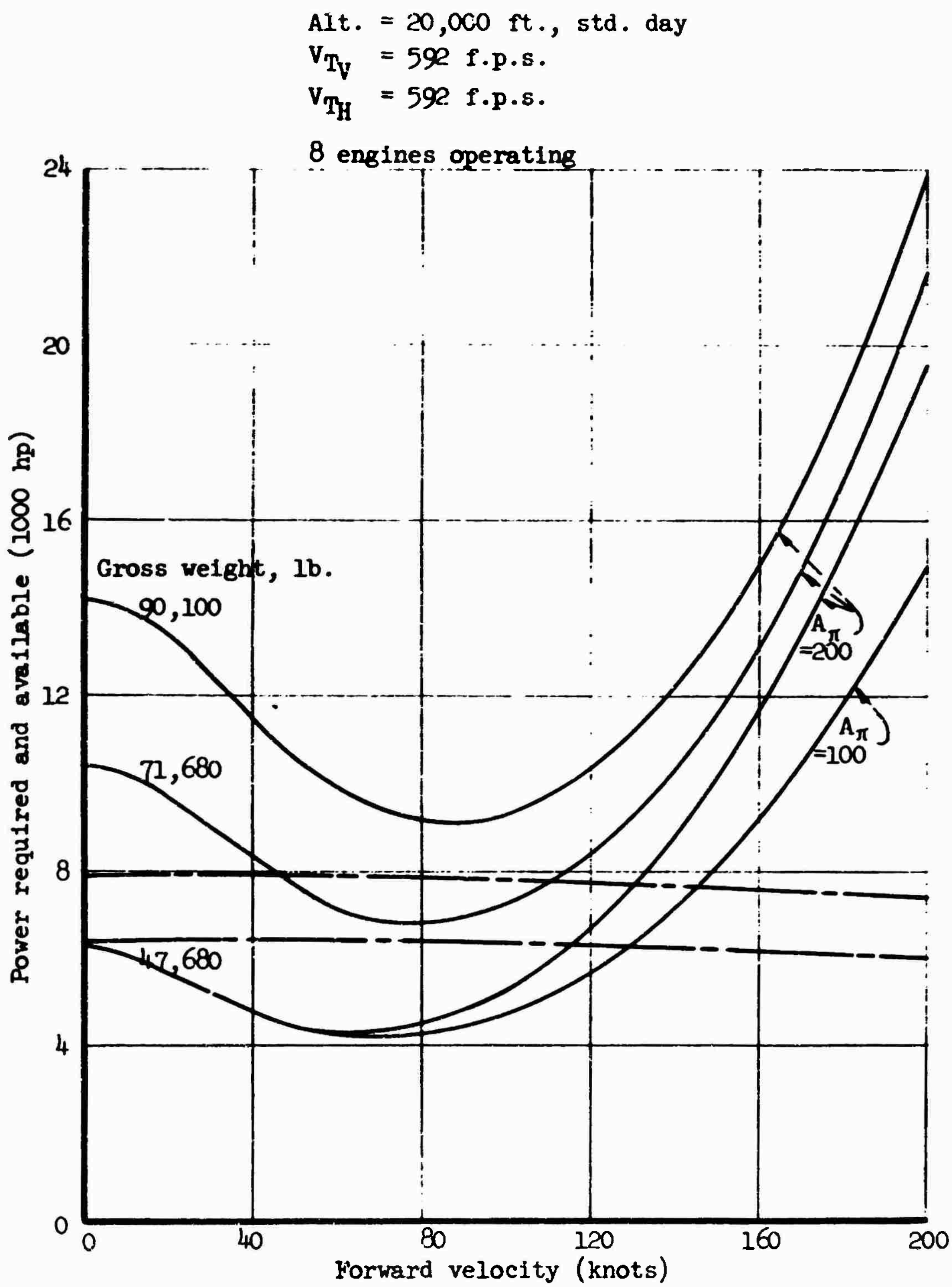

Figure 10a. Power Required and Available Versus Forward Velocity - 20,000 Ft. Altitude.

<u>5.0 POWER AVAILABLE</u>

The power plant selected for the Model 1108 is the Continental Model 357-1 turbojet engine. The engine ratings utilized in developing the data presented in this section are as follows:

Military rated thrust	1,540 lb.	At V_T = 650 ft/sec.
Normal rated thrust	1,170 lb.	

The method of establishing engine power available at altitude and for off-standard conditions is by the procedures developed in the parametric study and those outlined in the engine manufacturer's specification, Reference 5; namely,

a) Power available for hover (standard day):

$$P_{a_H} = \frac{F_n V_{T_H} n_e}{550} \qquad (21)$$

where: F_n = rated thrust at ambient conditions and hover tip speed, lb. (ref. Figures 1 through 4)
V_{T_H} = hover tip speed
n_e = number of engines

b) Power available for forward flight (standard day):

$$P_{a_V} = P_{a_H} - \frac{V^2 W_a n_e}{(32.2)(1,100)} \quad \begin{Bmatrix}\text{Ref. 7,}\\ \text{Eq. 54}\end{Bmatrix} \qquad (22)$$

where: P_{a_H} = power available for hover at a predetermined altitude
V = forward velocity, f.p.s.
W_a = air flow through engine, lb/sec. (manufacturer's specification)
n_e = number of engines

Curves of power available versus altitude for both normal and military rated power, at standard atmosphere conditions, are presented in Figure 11. These engine curves are based on the following assumptions:

a) Zero exhaust losses
b) ICAO standard pressure at each altitude
c) No induction air contamination
d) Zero power losses due to yawing and/or pitching angle of the engines
    1) air inflow variations
    2) fuel variations

The curves of Figure 11 were then cross-plotted and power available versus forward speed presented in Figure 12.

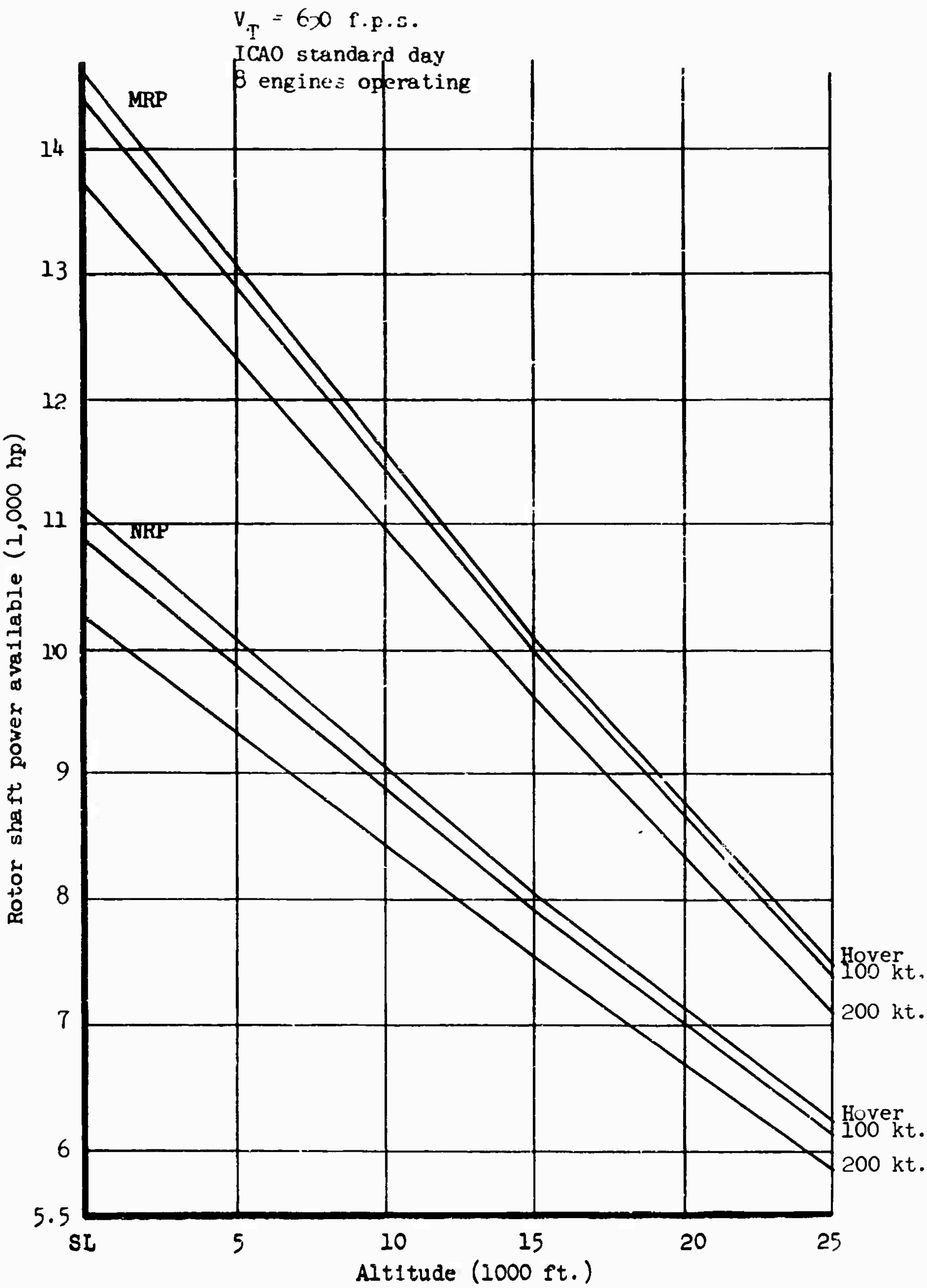

Figure 11. Power Available Versus Altitude.

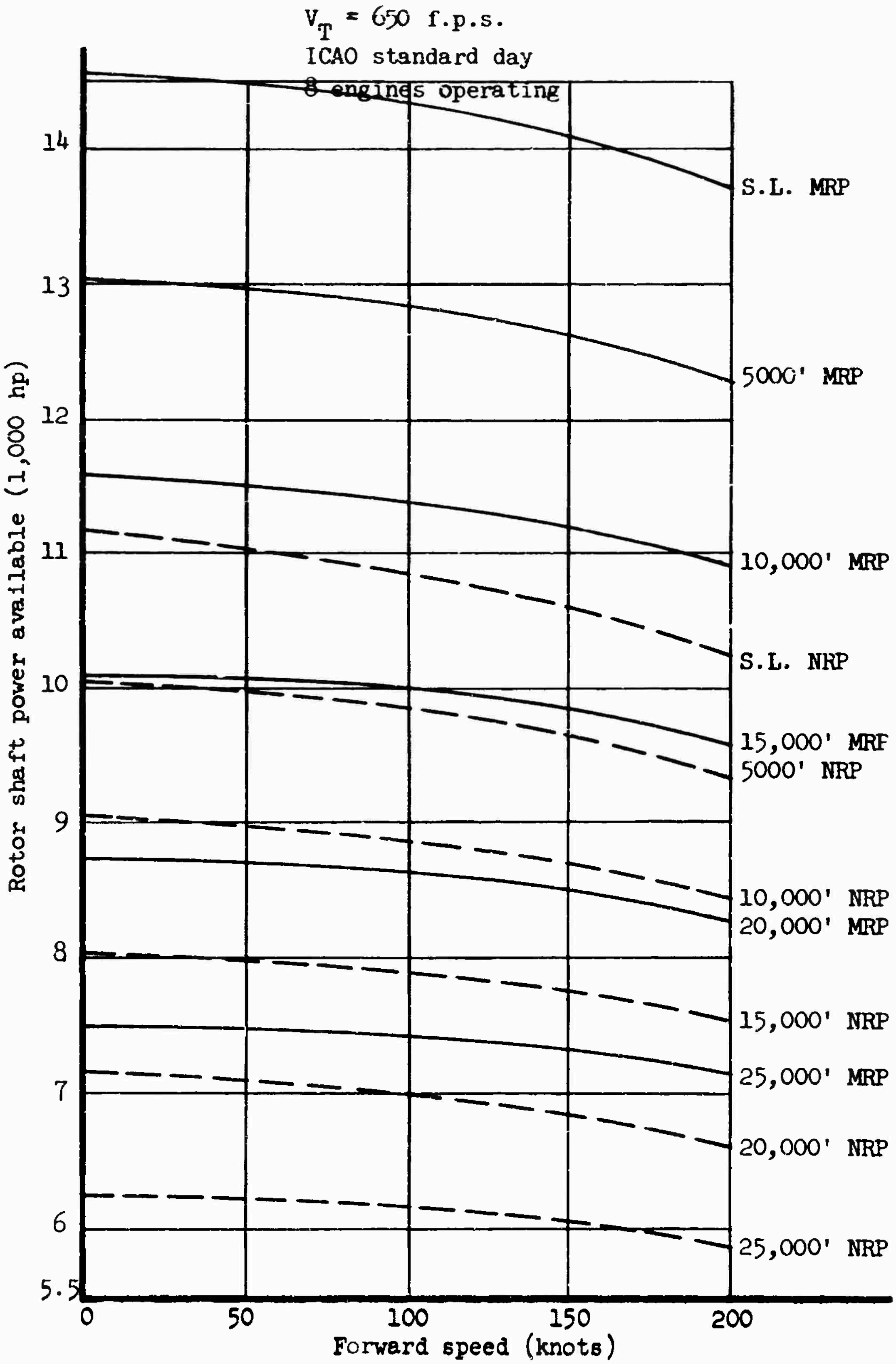

Figure 12. Power Available Versus Forward Speed.

6.0 PERFORMANCE CHARACTERISTICS

6.1 Specification Required Performance

6.1.1 Hover Ceiling

From the mission description, as presented in the statement of work, Reference 2, the specified hover ceiling requirement is that the helicopter be capable of hovering out-of-ground effect at design gross weight on military rated power at 6,000 feet, 95°F.

A temperature of 95°F. at 6,000 feet corresponds to 57.4°F. over standard temperature. For purposes of calculating a density ratio, the standard ICAO pressure-altitude relationship is used. Therefore, for reference, the equivalent density ratio at 6,000 feet, 95°F. is $\rho/\rho_o = .7495$.

The hot day hover ceiling is most simply determined by calculating the power required for selected altitudes at the equivalent density ratio; i.e., the density ratio corresponding to the combination of standard pressure and temperature of standard plus 57.4°F.

$$\rho/\rho_o = \frac{P_{std}}{\rho_o gR(T_{std} + 57.4)}$$

The curve then obtained is a plot of power required for a condition of 57.4°F. overstandard temperature versus altitude. Superimposed on this same plot is the engine power available for the same temperature condition. The intersection of the two curves is then the limiting hover ceiling out-of-ground effect. These curves are presented in Figure 13.

Sample calculation: Hover, OGE, 6,000 feet, 95°F. at 71,680 pounds.

From Sections 4.1 and 4.2, the power required to hover at sea level, OGE, on a standard day is:

$$rhp_H = 1.031\left[\frac{1.13(W)\frac{1}{B}\sqrt{\frac{W}{2\rho_o}}(K_\mu)}{550} + (200021.04\delta_{m_B}K_{\mu_b} + 5039.57\delta_{m_T}K_{\mu_N})\right] + 100$$

Substituting B = .964 and rewriting this equation to reflect the affect of the overstandard temperature condition gives

$$rhp_H = 1.031\left[\frac{1.172W\sqrt{\frac{W}{2\rho_o}}(K_\mu)\sqrt{\frac{\rho_o}{\rho}}}{550} + (200021.04\delta_{m_B}K_{\mu_b} + 5039.57\delta_{m_T}K_{\mu_N})\frac{\rho}{\rho_o}\right] + 100 \tag{23}$$

$$K_\mu = 1.00 \text{ (Figure 1)}$$
$$w = 7.3 \text{ (Section 2.2)}$$
$$\rho_o = .002378$$
$$\rho/\rho_o = .7495$$
$$K_{\mu_b} = 1.00 \text{ (Section 4.2)}$$
$$K_{\mu_N} = 1.00 \text{ (Section 4.2)}$$
$$\delta_{m_b} = .009 + .00927 C_{L_{r_o}}^2 (\rho_o/\rho)^2 = .009 + .00927(.3296)^2(1/.7495)^2$$
$$= .009 + .00178 = .01078$$
$$\delta_{m_I} = .282 + .1 C_{L_{r_o}}^2 (\rho_o/\rho)^2 = .282 + .1(.3296)^2(1/.7495)^2$$
$$= .282 + .01915 = .30115$$

$$rhp_H = 1.031 \left\{ \frac{1.172(71,680)\sqrt{\frac{7.3}{.004756}}\sqrt{\frac{1}{.7495}}}{550} + \left[(200,021)(.01078) + (5,039.57)(.30115)\right](.7495) \right\} + 100 = 1.031(6,911.8 + 2,753.6) + 100$$
$$= 9,965 + 100 = 10,065 \text{ hp}$$

The hover ceiling out-of-ground effect for standard ICAO conditions is determined in the same manner and is presented versus gross weight in Figure 14.

While not required, the hover ceiling in-ground effect for standard ICAO conditions is also presented for purposes of performance comparison. When a rotor is positioned such that the wake impinges on a surface, the surface influences the performance of the rotor through its restraint of the rotor downwash. As the rotor approaches the ground plane, the induced velocity required to produce a given thrust is reduced, with a resultant decrease in the induced power. The rotor height above the ground, z, for in-ground effect hovering performance is the sum of the distance between the main rotor teetering point and the rest gear, and the rest gear and the ground. The first value is fixed by the design of the helicopter, the second is determined from flight test as the minimum height at which the helicopter can safely translate into forward flight. This transition region is primarily dependent upon rotor inertia, lift coefficient, and engine power characteristics. For the purpose of this analysis, a $z/D = .29$ (a wheel height above the ground equal to 5 feet) will be assumed.

The results of the analysis of the ground effect on power may be summarized in a single plot representing the ratio of the power required in effect to that required in free air against height above the ground for the condition of constant thrust coefficient, C_T/σ^2.

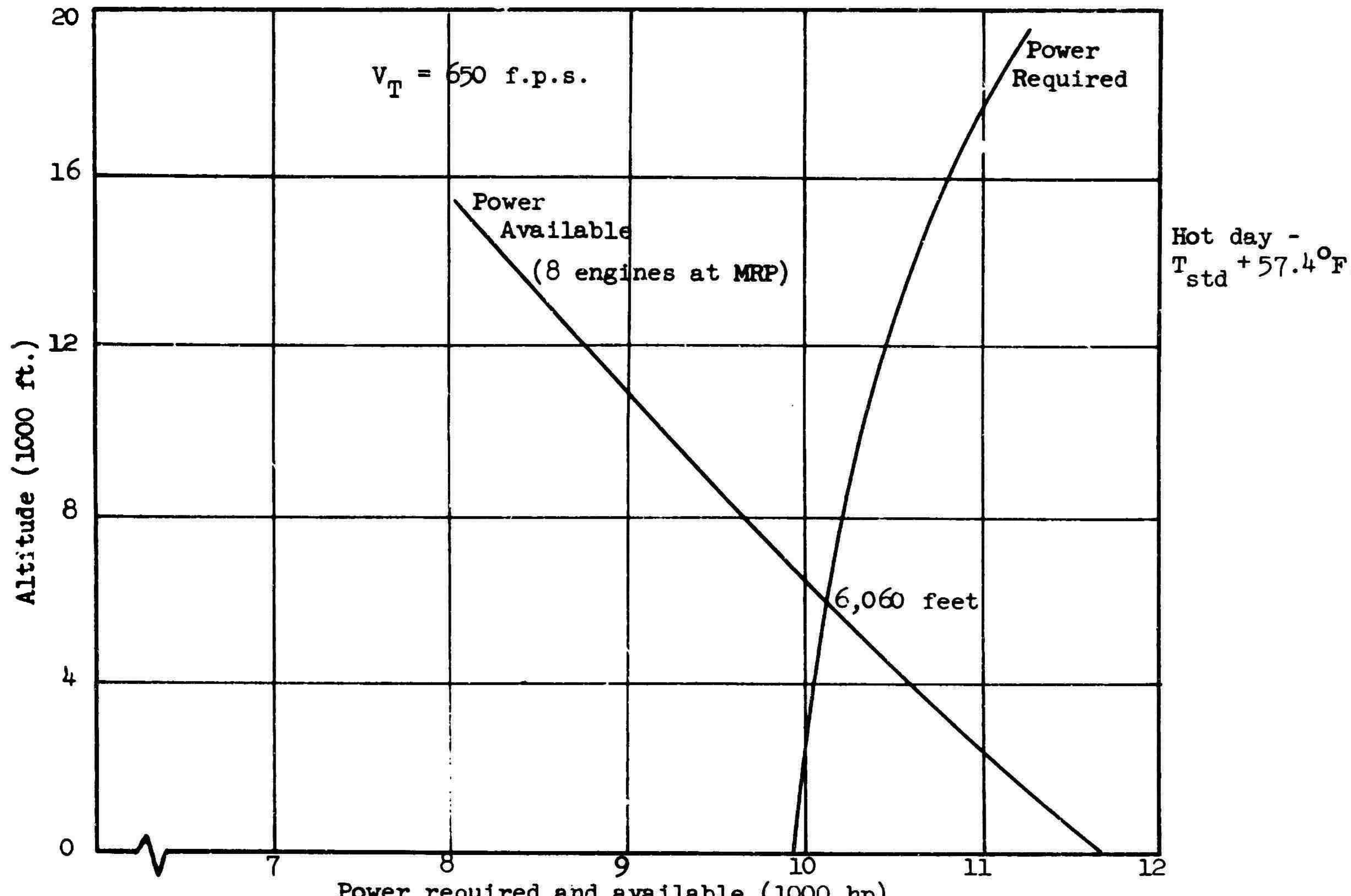

Figure 13. Hover Power Required Out-of-Ground Effect.

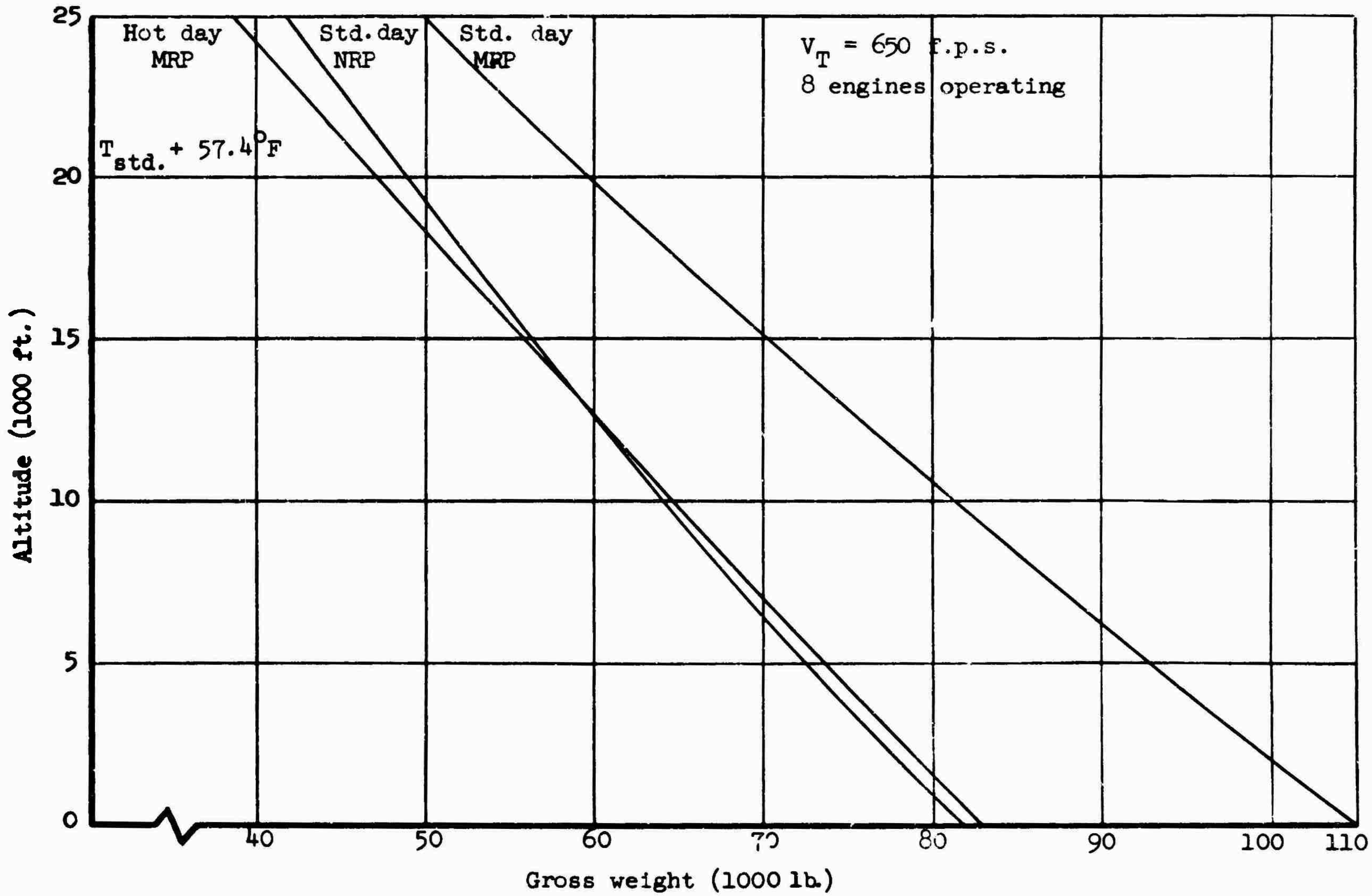

Figure 14. Hover Ceiling Out-of-Ground Effect Versus Gross Weight.

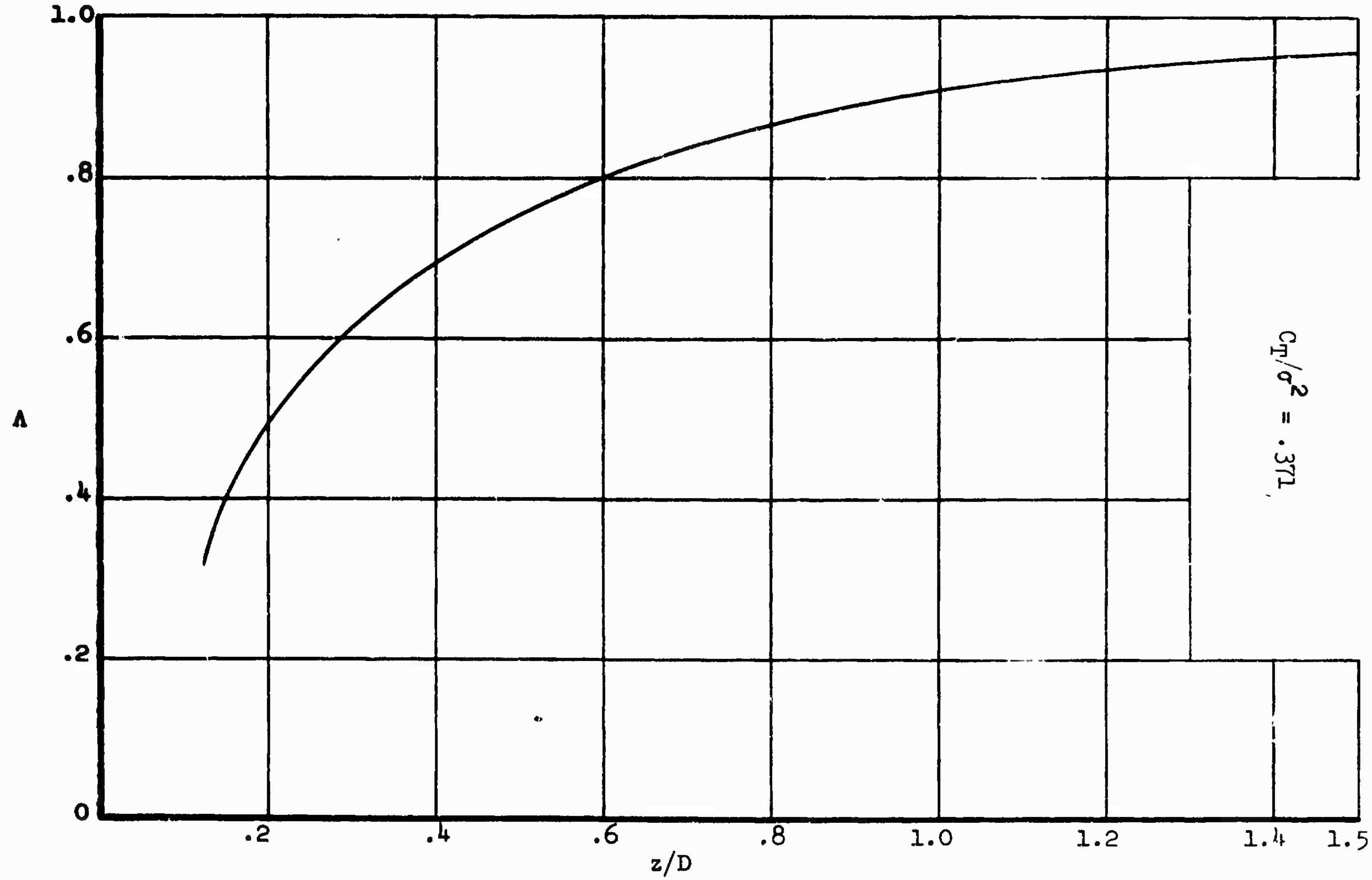

Figure 15. Induced Power Correction Factor Versus z/D - In-Ground Effect.

V_T = 650 f.p.s.
Standard day
8 engines operating

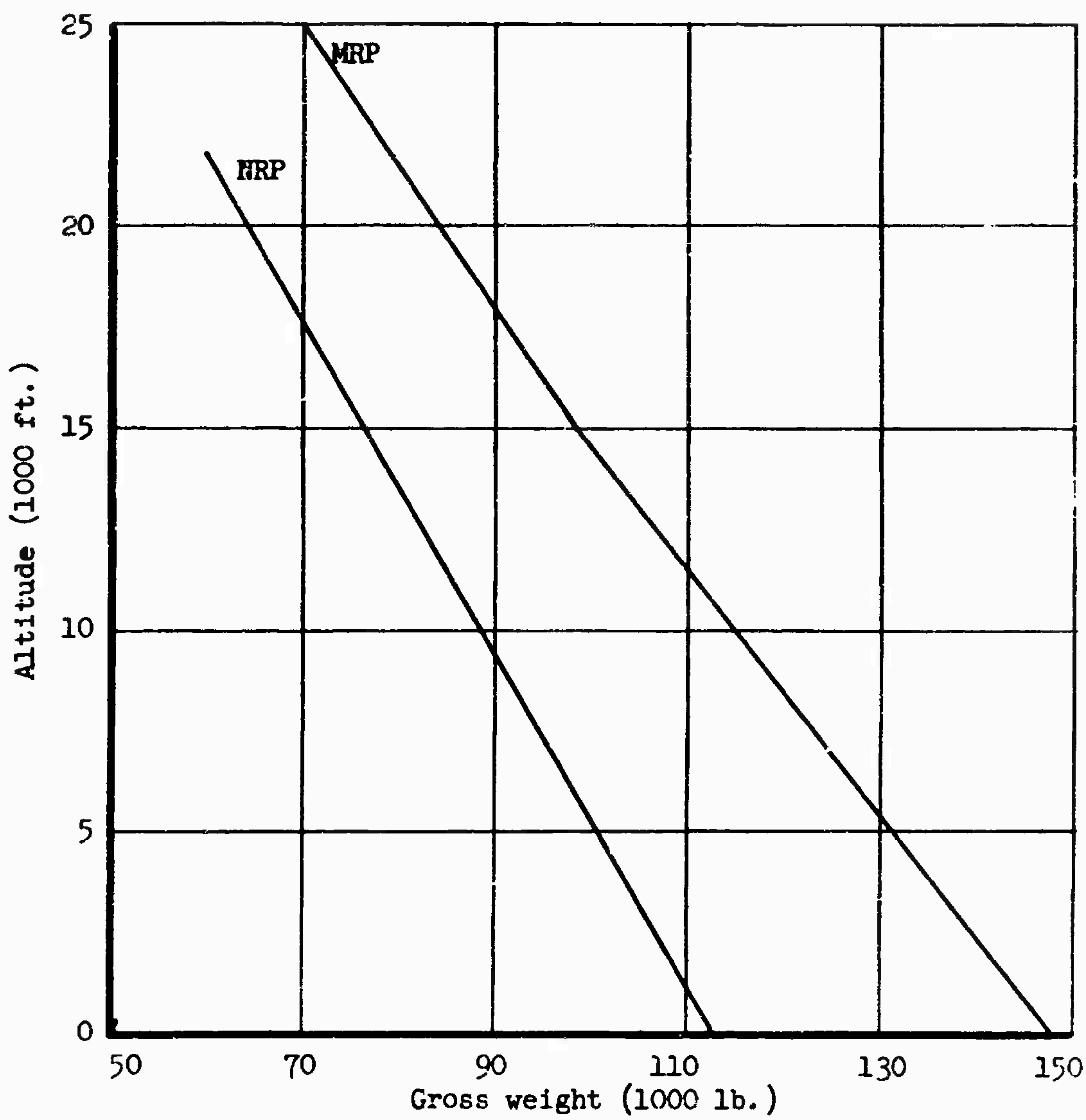

Figure 16. Hover Ceiling In-Ground Effect Versus Gross Weight - Standard Day.

For purposes of plotting it is convenient to relate the total rotor height above the ground to the diameter by the ratio, z/D, in the determination of the induced power correction factor, Λ, where

$$\Lambda = ihp_{IGE}/ihp_{OGE}$$

Figure 15 gives the variation of Λ with z/D for a rotor exhibiting those parameters recorded in Section 2.2 of this report; namely

$$C_{L_{r_o}} = .3296$$

$$\sigma = .14805$$

$$C_T = \frac{C_{L_{r_o}}(\sigma)}{6} = \frac{.3296(.14805)}{6} = .0081329$$

$$C_T/\sigma^2 = .0081329/.0219188 = .371$$

Reference 6 establishes the Λ to z/D relationship in its Figures 5 through 11 from which Figure 15 has been taken.

The determination of in-ground effect hovering power is the same as for out-of-ground effect with the exception that the induced power term alone is modified by the factor Λ = .60(Figure 15, z/D = .29). A plot of hover ceiling in-ground effect versus gross weight is presented in Figure 16.

6.1.2 Airspeed-Altitude Limits

The rotor parameters for the tip turbojet rotor system were carefully selected to preclude the possibility of premature blade tip stall and drag divergence. Blade parameters which determine stall and drag limits are airfoil section, blade twist, solidity (blade chord), and tip speed. The main rotor airfoil section used, NACA 0015, has a nominal stall angle of 12 degrees. Sufficient blade chord, combined with the selected tip speed, must be used to keep blade angles of attack below this limit. Excessive chord, however, results in a power limit in forward speed due to an increase in rotor profile power.

The selection of tip speed is primarily based on high-speed requirements wherein the rotor tip speed must be high enough to prevent stall on the retreating blade, yet not high enough to create drag divergence on the advancing blade. There are secondary considerations which influence the final selection. These are autorotation flare characteristics and required tail rotor power. The autorotation flare characteristics, assuming a fixed diameter, become more favorable with increasing tip speed due to increased rotor kinetic energy. In the final analysis, where there is a family of tip speed-solidity combinations which will satisfy the power and rotor blade limits, the higher tip speeds are generally favored.

The selection of the proper blade twist is primarily based on selecting a value which will reduce the retreating blade angle of attack to a value equal to or less than the stall angle. The blade twist angle is a unique parameter in that it is independent of any of the power-required terms. Therefore, in the blade tip stall and drag divergence analysis, if the range of tip speed and solidity values is very limited due to power limitations, blade twist may be independently varied to attain the desired blade tip angles. Actually, blade twist has, according to Reference 6, a beneficial effect on the induced power. The effect of twist is to modify the inflow distribution from triangular to a more uniform distribution. However, the net change in the induced power is very small; consequently, to be conservative it has not been considered in this analysis.

The equations for the tip angle of attack of the advancing and retreating blades are derived from blade element integrations of the elemental thrust and "flapwise" moment equilibrium expressions which are included as Part C of Appendix A of Reference 4.

Retreating blade tip:

$$\alpha_{(1)(270)} = A_1 C_{L_r} + A_2 \lambda + A_3 \theta_E \qquad (24)$$

Advancing blade tip:

$$\alpha_{(1)(90)} = A_1' C_{L_r} + A_2' \lambda + A_3' \theta_E \qquad (25)$$

The constants A_n and A_n' are functions of μ and are plotted in Figure 17, and

C_{L_r} = mean blade lift coefficient

α_{stall} = stall angle of attack = 12^o

θ_E = blade twist (washout) = -10^o = $-.1745$ rad.

λ' = inflow ratio referred to the tip path plane (positive when the inflow is downward)

The inflow ratio, λ', is the ratio of the total axial inflow to the blade tip speed and is expressed by

$$\lambda' = \frac{u_i + u_R + u_p}{V_T} \qquad (26)$$

The terms u_R and u_p are essentially equivalent inflow velocities. The u_R term is the inflow to the rotor due to tilt to overcome the rotor profile drag and u_p is the inflow to the rotor due to tilt to overcome the fuselage parasite drag. Combined, they are the additional increment of inflow necessary, when the rotor is tilted, to increase the resultant rotor thrust such that the vertical component of thrust is equal to the weight.

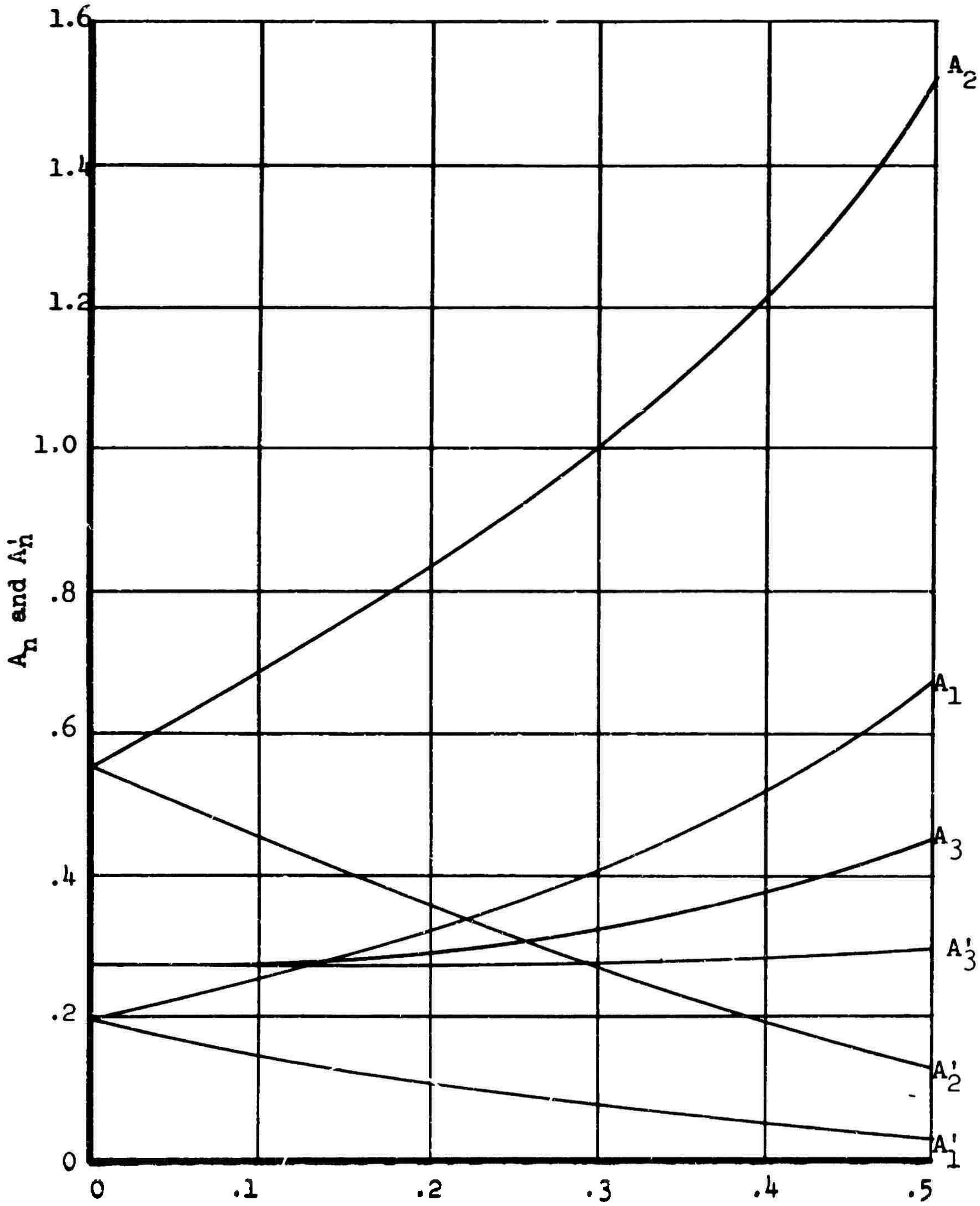

Figure 17. Constants in the Expression for Blade Tip Angle of Attack at $\psi = 90^\circ$ and $\psi = 270^\circ$ Versus Tip Speed Ratio, μ.

From Equation (8):

$$u_i = \frac{1.13}{B}\sqrt{\frac{W}{2\rho}}\,(K_\mu) \qquad (27)$$

and by definition,

$$u_R = \frac{1100}{W}\,(Rhp_H)\mu^2 \qquad (28)$$

$$u_p = \frac{550}{W}\,(php) \qquad (29)$$

The above expressions are put in tabular form and values of λ' calculated at selected altitudes and forward speeds. These values are then substituted in Equations (24) and (25) from which the tip angles of attack at the selected airspeeds and altitudes, are computed. Tip stall limits are then established by plotting the retreating blade angle of attack versus altitude for selected forward velocities, the limiting angle being 12^o. This data was then cross-plotted as altitude versus forward velocity, Figures 18 through 20.

The compressibility limits on forward velocity are determined from the curve of Figure 13, Reference 4, included herein as Figure 21. Figure 21 presents the variation of drag divergence Mach number with blade section angle of attack. The curve is representative of an NACA 0015 airfoil and is based on actual test data from several sources. Calculated performance limits for current Hiller rotorcraft, based on this curve, show good agreement with flight test data. The actual Mach number, M, is calculated for each of the selected altitudes and forward velocities from the expression

$$M_\psi = \frac{V_T \pm V}{a} \qquad (30)$$

where "a" is the speed of sound at altitude. The actual Mach number data is superimposed on the same figure, and the resulting intersections are the compressibility limits. These intersections were then cross-plotted as altitude versus airspeed, Figures 18 through 20. While advancing blade compressibility does not form one of the altitude limits, it is shown for purposes of comparison.

A third limit is introduced which is the power limit. The resulting power limit curves (normal and military rating) are derived by plotting the maximum and minimum power limit forward velocities, as determined from the power required curves, versus altitude.

The three limits, tip stall, compressibility, and power, are plotted together for each of the gross weight conditions (W = 47,680 pounds, 71,680 pounds, and 90,100 pounds), in Figures 18 through 20. Their resultant intersections then form the airspeed-altitude limits (performance envelope of the helicopter).

Note: All power limits based on 8 engines operating.
Standard ICAO conditions.

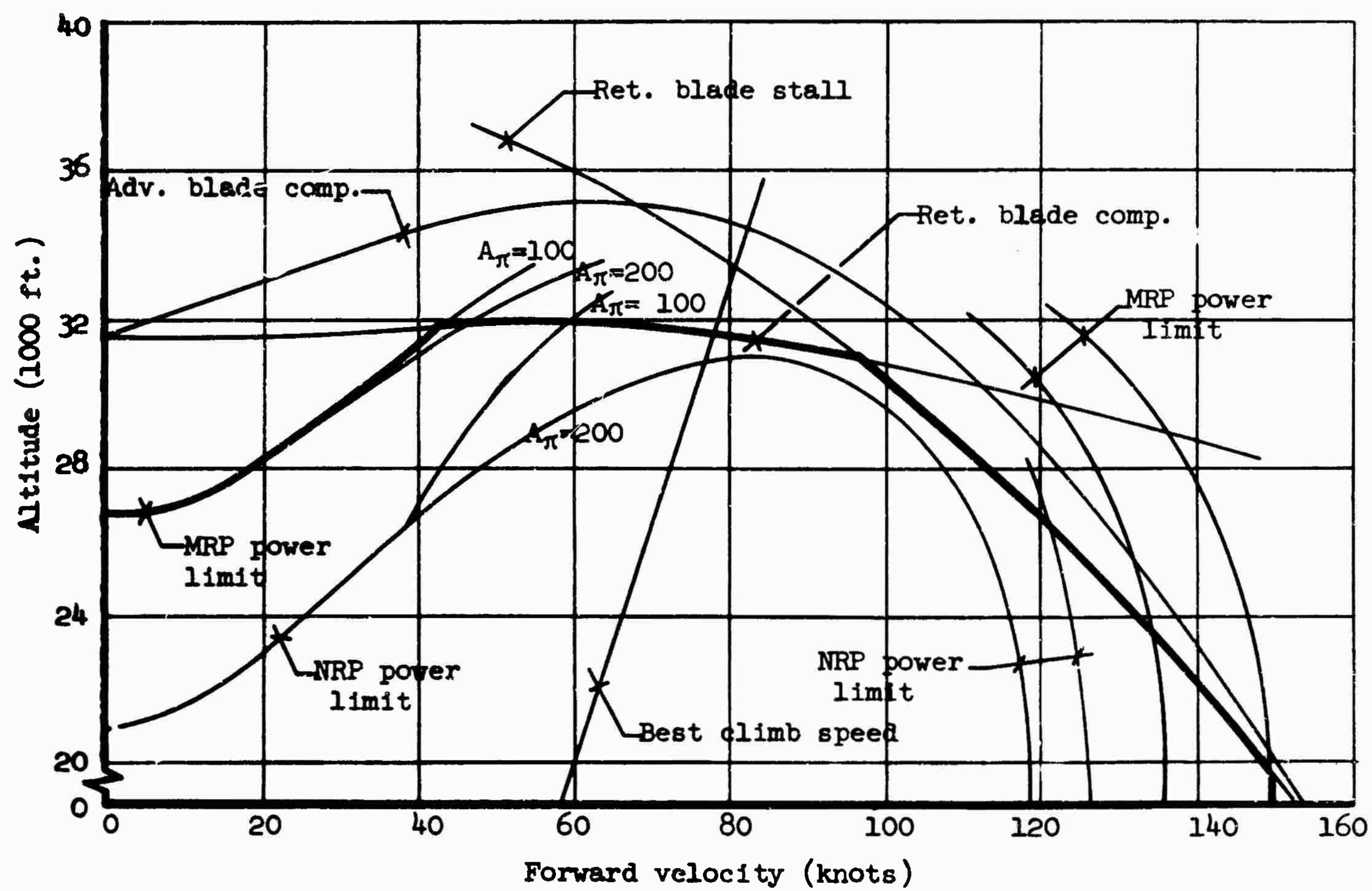

Figure 18. Airspeed-Altitude Limits - 47,680 Lb. Gross Weight.

Note: All power limits based on 8 engines operating.
Standard ICAO conditions.

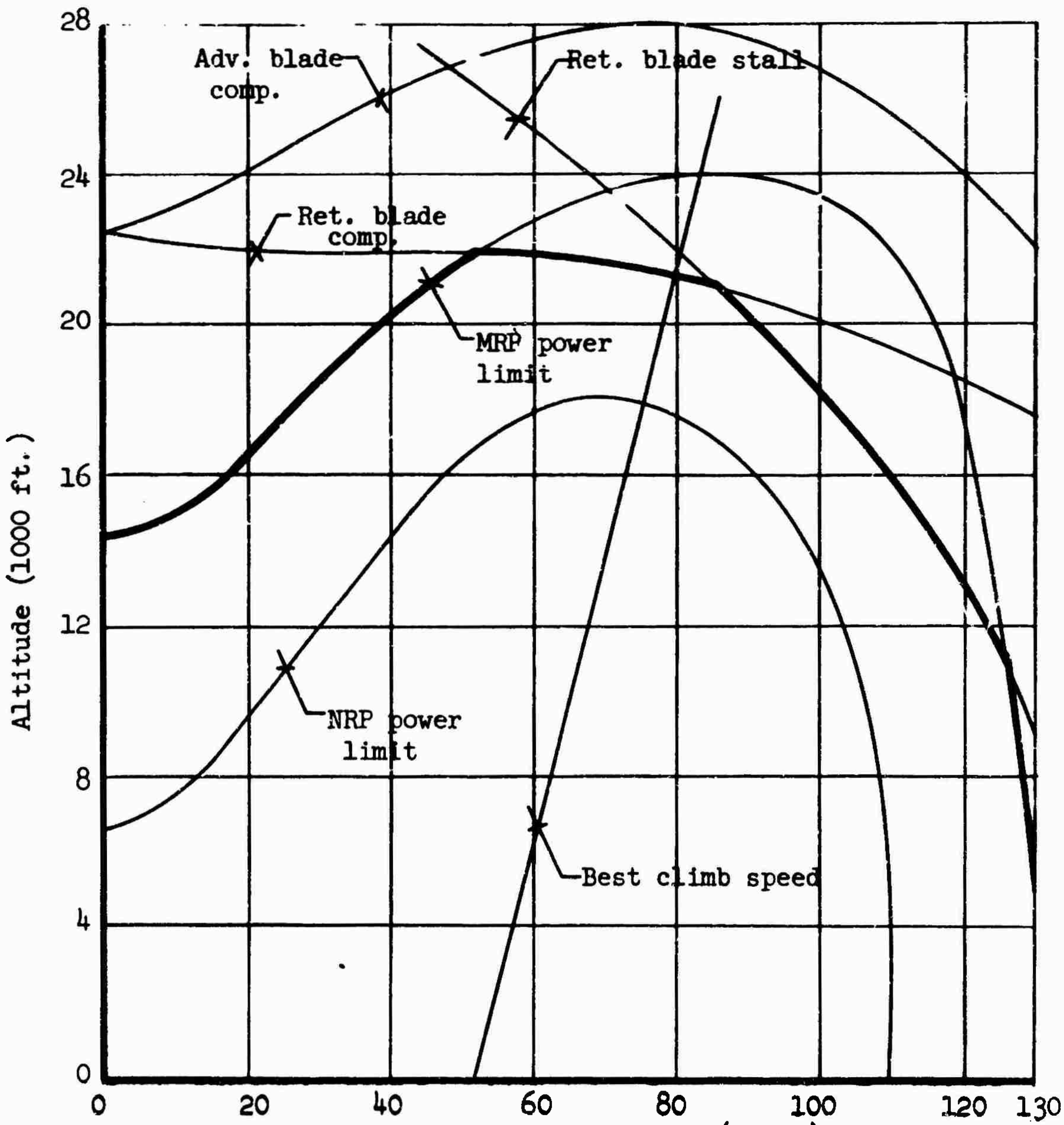

Figure 19. Airspeed-Altitude Limits - 71,680 Lb. Gross Weight.

Note: All power limits based on 8 engines operating.

Standard ICAO conditions.

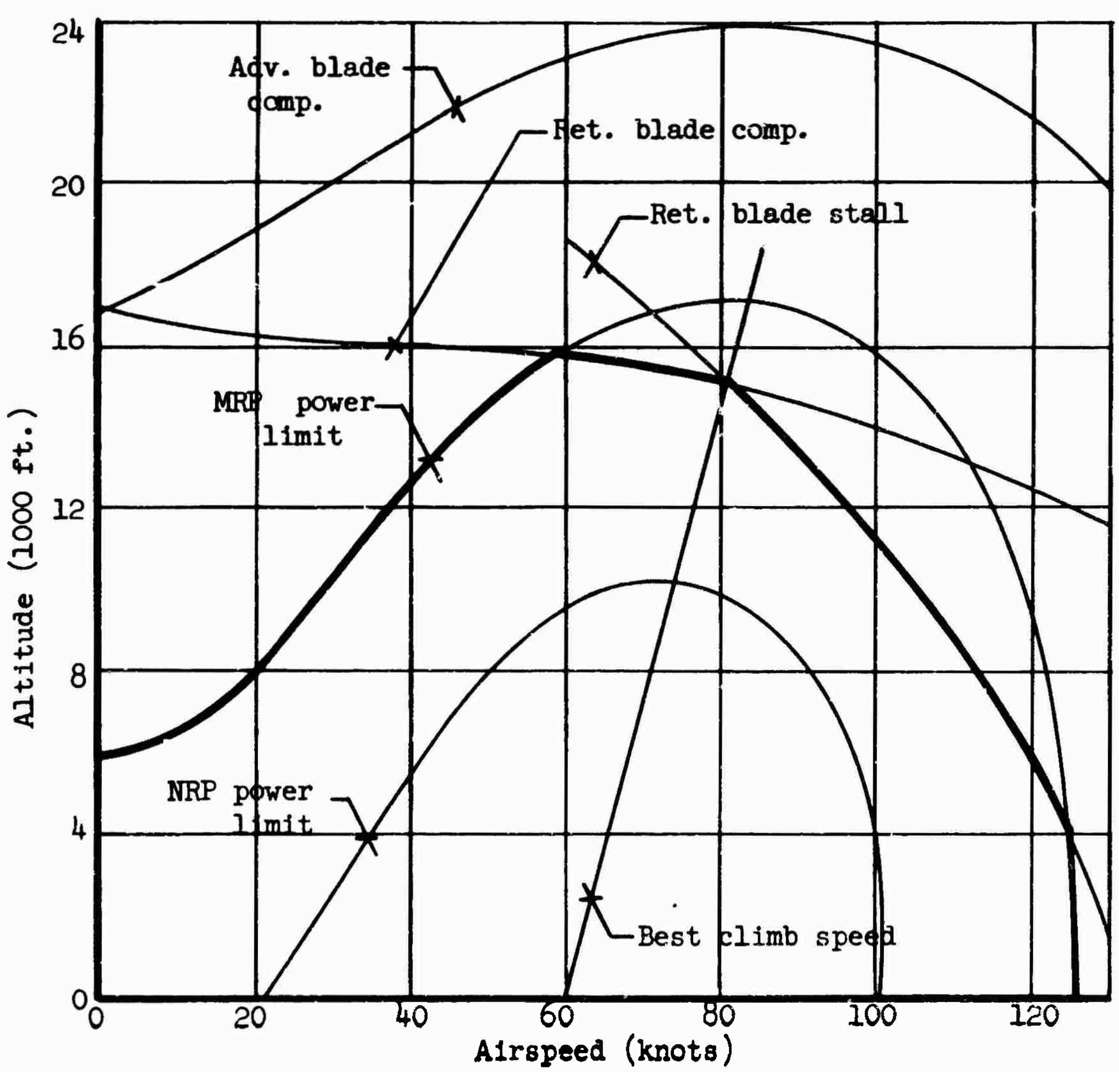

Figure 20. Airspeed-Altitude Limits - 90,100 Lb. Gross Weight.

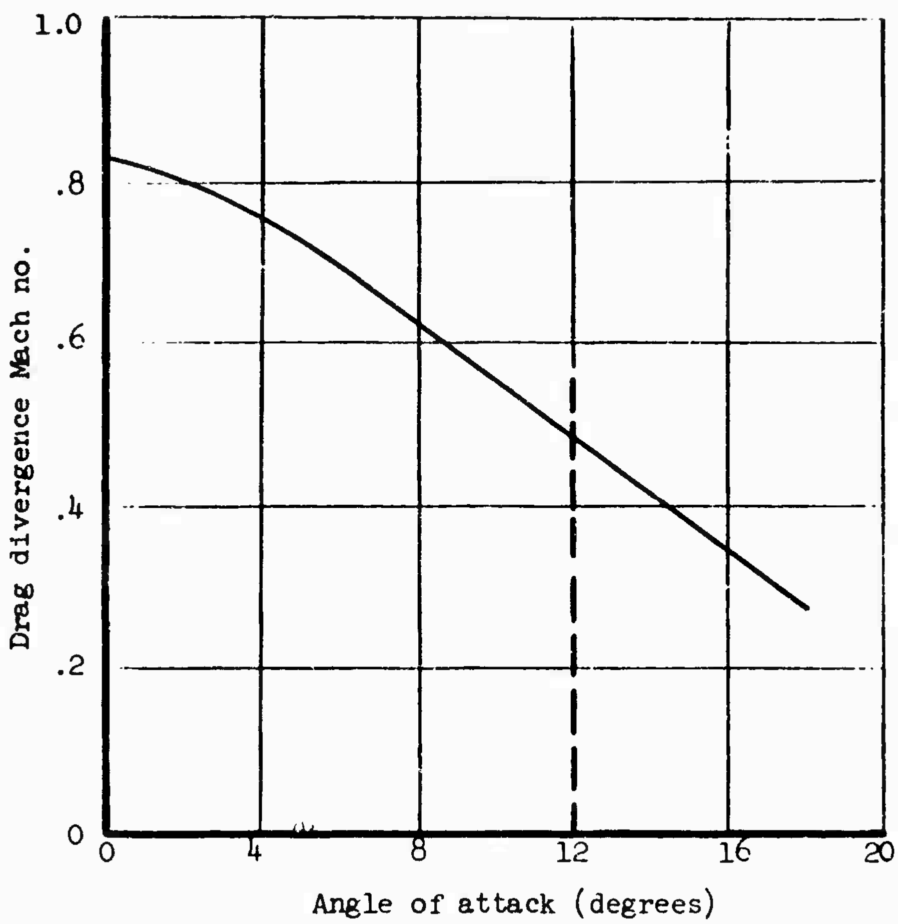

Figure 21. Estimated Drag Divergence Mach No. Versus Blade Tip Angle of Attack for NACA 0015 Airfoil.

For the design gross weight condition of 71,680 pounds, Figure 19, the performance envelope is outlined by the heavy line. Figure 19 shows that the tip turbine is power limited at sea level at 130 knots. This power limit extends to 11,000 feet at which point the maximum forward velocity decreases slightly to 126 knots due to the engine derating. At 11,000 feet the power limit curve intersects the retreating blade stall limit curve and the speed is limited by blade stall to 21,000 feet. From 21,000 feet to 22,000 feet the speed is limited by retreating blade compressibility at which point it again intersects the power limit curve which goes to zero forward velocity at the out-of-ground effect hover ceiling of 14,400 feet. In all cases, as shown, the advancing blade compressibility limiting curve falls outside of the performance envelope.

6.1.3 Mission

As defined by Reference 2, the mission description is as follows:

a) Payload (outbound) - 12 tons
b) Radius - 50 nautical miles
c) Cruising speed:
   1) outbound - 60 knots
   2) inbound (no payload) - 100 knots
d) Takeoff and destination elevation - sea level
e) Cruising altitude - sea level
f) Atmospheric condition - sea level, standard atmosphere
g) Hovering time (out-of-ground effect):
   1) at takeoff - 3 minutes
   2) at destination - 2 minutes
h) Reserve fuel (percent of initial fuel) - 10 percent

In order to maximize range, the specific range (nautical miles per pound) is plotted versus forward velocity, Figure 22. This plot is constructed by reading the specific fuel consumption for selected values of percent of normal rated power (derived from power requirements at specific forward velocities as found in Figures 6 through 10a) from Figure 23, then substituting this value, the appropriate forward velocity, and required horsepower into the following expression, solving for the specific range and plotting the results.

$$\text{Specific range} = \frac{V_{kts}}{(BSFC)(rhp)} \tag{31}$$

From the specific range curves of Figure 22 the points of zero slope were determined and cross-plotted on Figures 24 and 25 as specific range versus gross weight and best cruise speed versus gross weight. As specific range, gross weight, cruising speed, and time are all interrelated, the fuel required for the mission is an integral problem. It has been found sufficiently accurate to use average values for the mission phases. Using this assumption, the mission capability may be determined in the following manner.

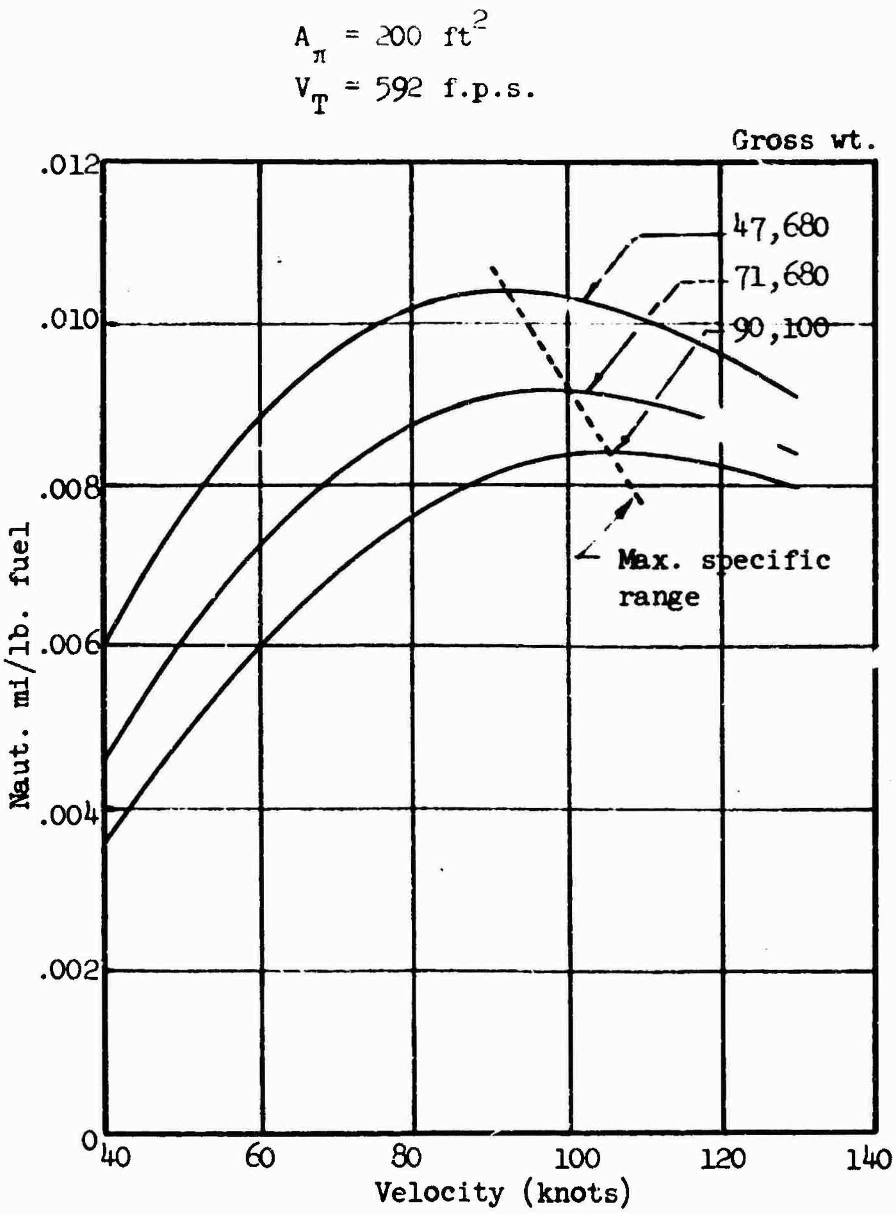

Figure 22. Specific Range Versus Forward Velocity at Sea Level, Standard Day.

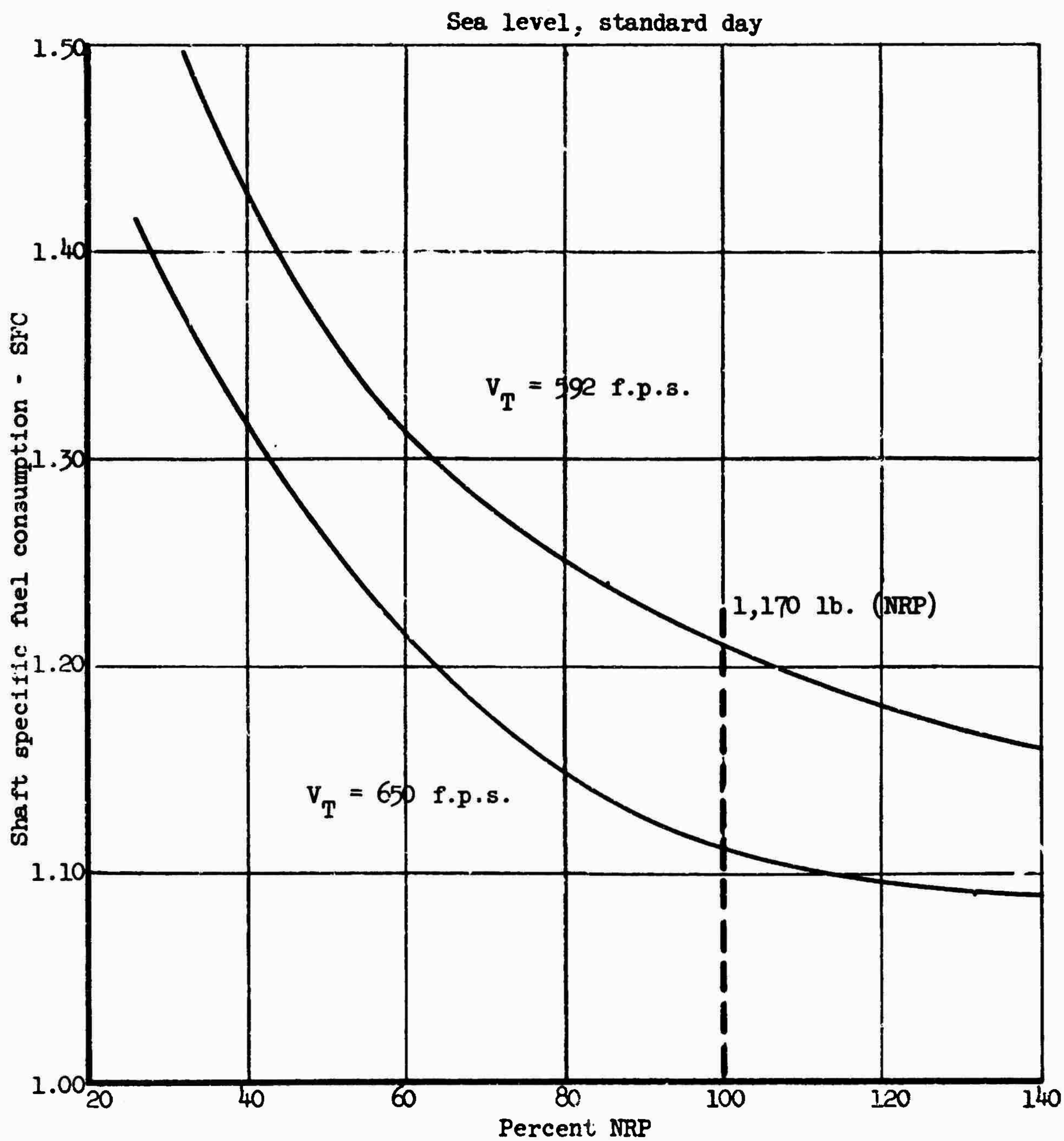

Figure 23. Shaft Specific Fuel Consumption Versus Normal Rated Power.

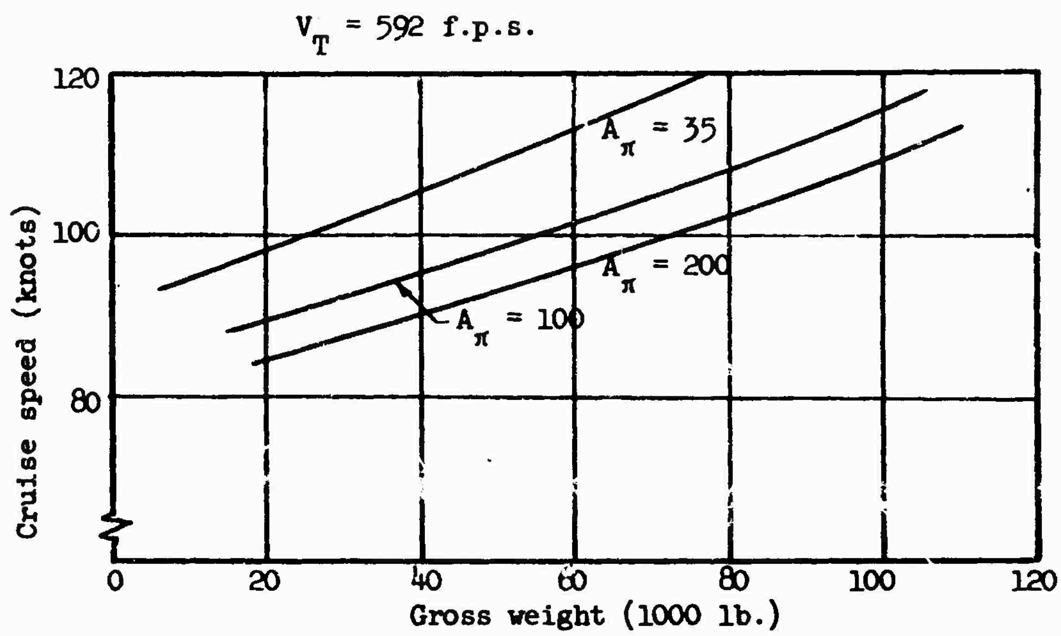

Figure 24. Best Cruise Speed Versus Gross Weight at Sea Level, Standard Day.

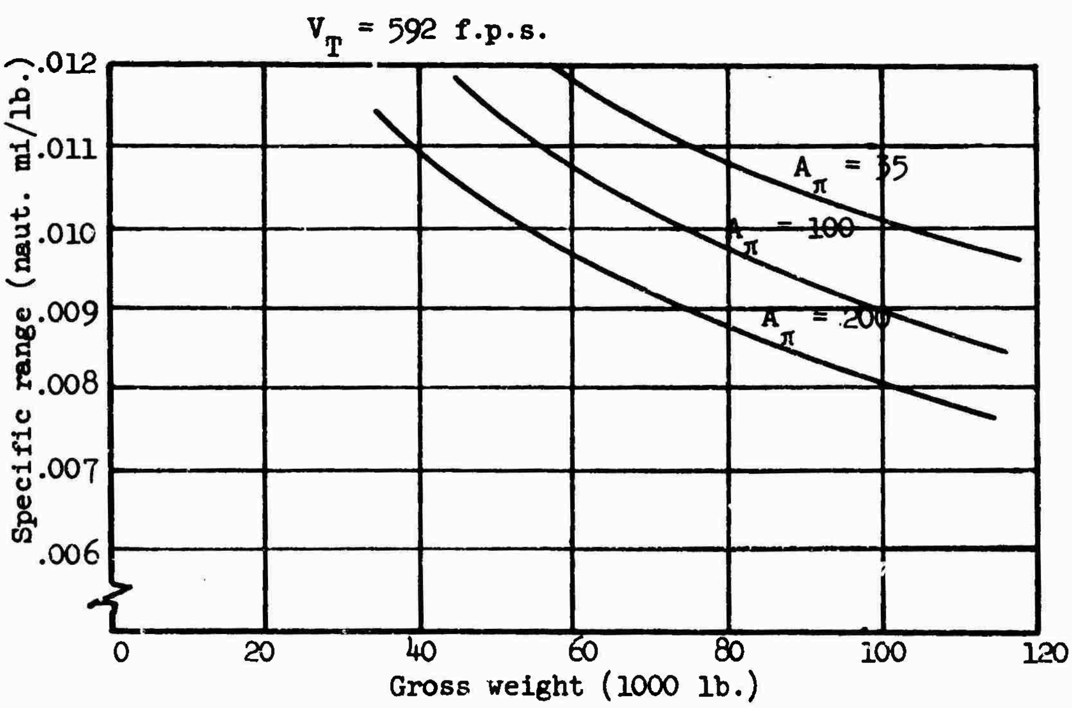

Figure 25. Specific Range Versus Gross Weight at Sea Level, Standard Day.

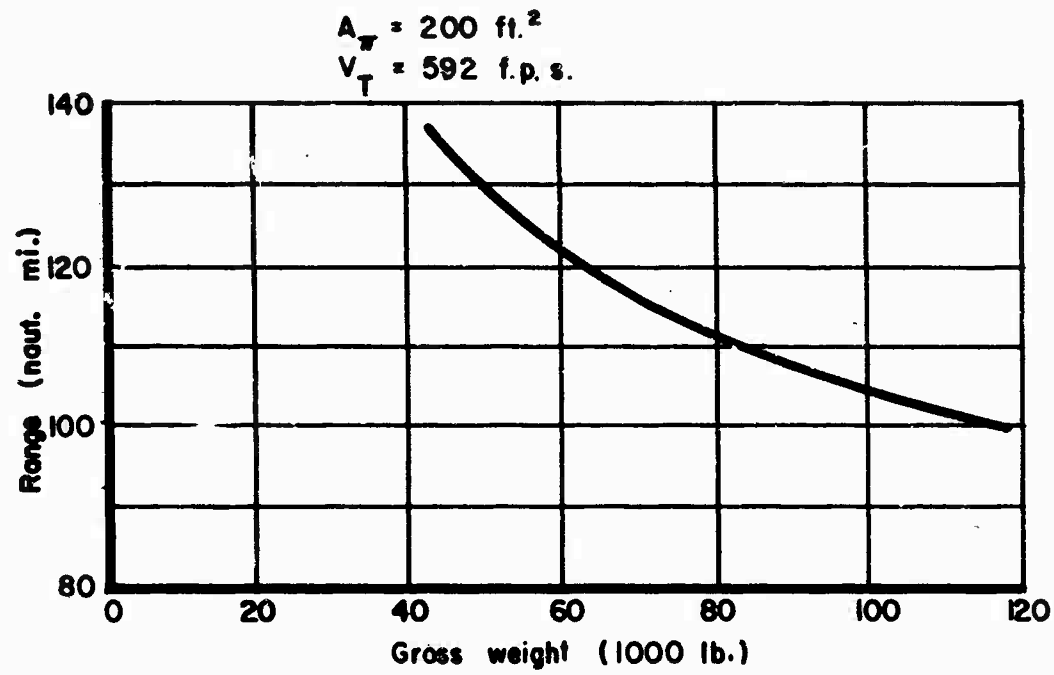

Figure 25a. Range Versus Take-Off Gross Weight at Sea Level, Standard Day. Includes 10 Percent Initial Fuel Reserve.

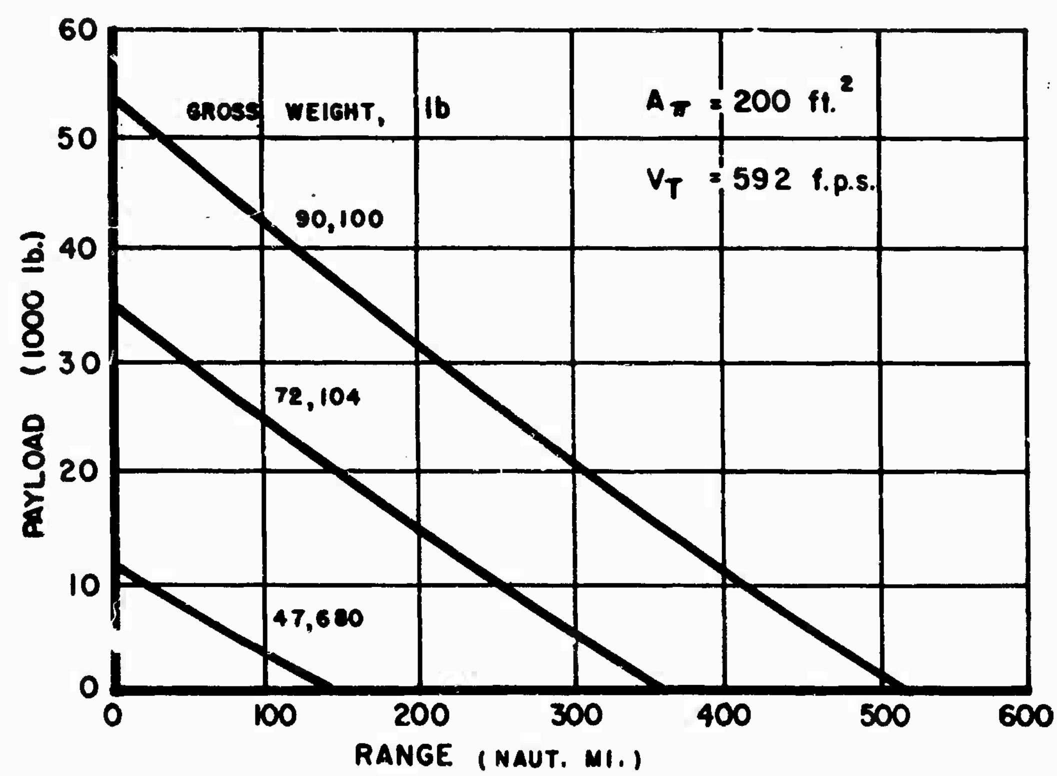

Figure 25b. Range Versus Payload at Sea Level, Standard Day.

Schematically, the mission, as defined above, may be expressed as follows:

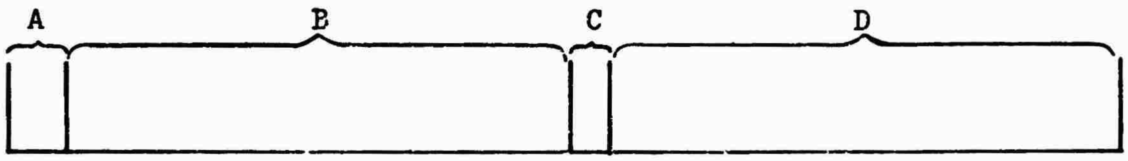

A) Hover at take-off - 3 minutes
   1) Initial gross weight - 72,104 pounds (includes fuel, fuel tanks, and 12-ton payload)

B) Outbound leg - 50 naut. miles at V = 60 knots

C) Hover at destination - 2 minutes; drop 12-ton payload

D) Inbound leg - 50 naut. miles at V = 100 knots

Note: The mission is to be flown with all of the eight engines operating. Although engine shut down was considered in the parametric study, Reference 7, it was deemed advisable to present the performance analysis with all eight engines operating.

The average gross weight during each of the individual phases of the mission is determined in the following manner:

W_i = gross weight at the beginning of the mission phase being investigated.

W_F' = estimated fuel required to complete the mission phase under investigation at the initial gross weight, W_i.

Then,

$$W_{avg} = W_i - W_F'/2$$

The mission compliance capability is presented in Table 1. The results indicate a total fuel weight of 12,103 pounds or with a 10 percent reserve, a total fuel load of 13,434 pounds.

The parametric analysis, Reference 7, considered tubular type crane fuselage construction which was considered appropriate for very short range missions. Crane type fuselages of streamlined monocoque construction with lower drag have been investigated and found to provide large reductions of A_π without the external load. For a streamlined model crane an A_π of 35 square feet was calculated. Figures 24 and 25 show comparative increases of cruise speed and specific range over configurations with A_π equal to 100 and 200 square feet.

TABLE 1
MISSION COMPLIANCE

Phase	Starting Weight (lb.)	Fuel Used (lb.)	Finish Weight (lb.)	Duration
A	72,104	562	71,542	3 minutes
B	71,542	6,855	64,687	50 minutes
C	64,687	347	64,340	2 minutes
D	40,340	4,340	36,000	30 minutes
Total - 12,103 lb.				

Notes: V_T = 650 f.p.s. in hover.
V_T = 592 f.p.s. in forward flight.

8 engines operating at all times.

Increase in fuel flow at forward speeds taken into account (Section 3.3.2 and Figure 16 of Reference 7.)

Tail rotor requirements included.

6.2 Climb Performance

6.2.1 Maximum Rate of Climb

The maximum rate of climb is calculated from the standard energy expression:

$$R/C_{max} = \frac{33{,}000(\eta)(ahp - rhp_{min})}{W} \tag{32}$$

The power available for climb $(ahp - rhp_{min})$ is a maximum at the "bucket" or minimum point on the power required versus forward velocity curve. The value of η is established in Section 4.4. Maximum rate of climb values for both normal and military power at selected values of gross weight are plotted versus altitude in Figures 26 and 27. The sea level rate of climb is also cross-plotted versus gross weight for normal and military power in Figure 28.

Sample calculation: Maximum rate of climb, sea level at 71,680 pounds

ahp = 14,500 hp (NRP, Figure 12)

V_{climb} = 52.0 knots

η = .97 (Section 4.6)

rhp_{min} = 7380 hp

$$R/C_{max} = \frac{33{,}000(.97)(14{,}500 - 7{,}380)}{71{,}680} = 3{,}170 \text{ ft/min.}$$

It will be noted in Figures 26 and 27 that at altitude the rate of climb curves bend sharply as they approach zero rate of climb. This is due to retreating blade compressibility limiting the speed for best rate of climb. Referring to Figures 18 through 20, the speed for best rate of climb is shown as a curve increasing with altitude. However, using the design gross weight condition of 71,680 pounds as an example, from Figure 19 it is seen that at an altitude of 21,250 feet, the best climb speed curve intersects the retreating blade compressibility portion of the airspeed envelope. Therefore, above this altitude the helicopter must fly this indicated speed-altitude curve, and as a consequence, it is no longer flying at the speed, as shown on the power required curve, where the excess power is a maximum.

To calculate the compressibility portion of the climb versus altitude curve, it is then necessary above 21,250 feet to select a number of speed-altitude points from the airspeed envelope and determine the new excess climb power from the appropriate power required-altitude curve. Since these selected altitudes generally fall between the altitudes for which power required curves are presented, it is necessary to cross-plot

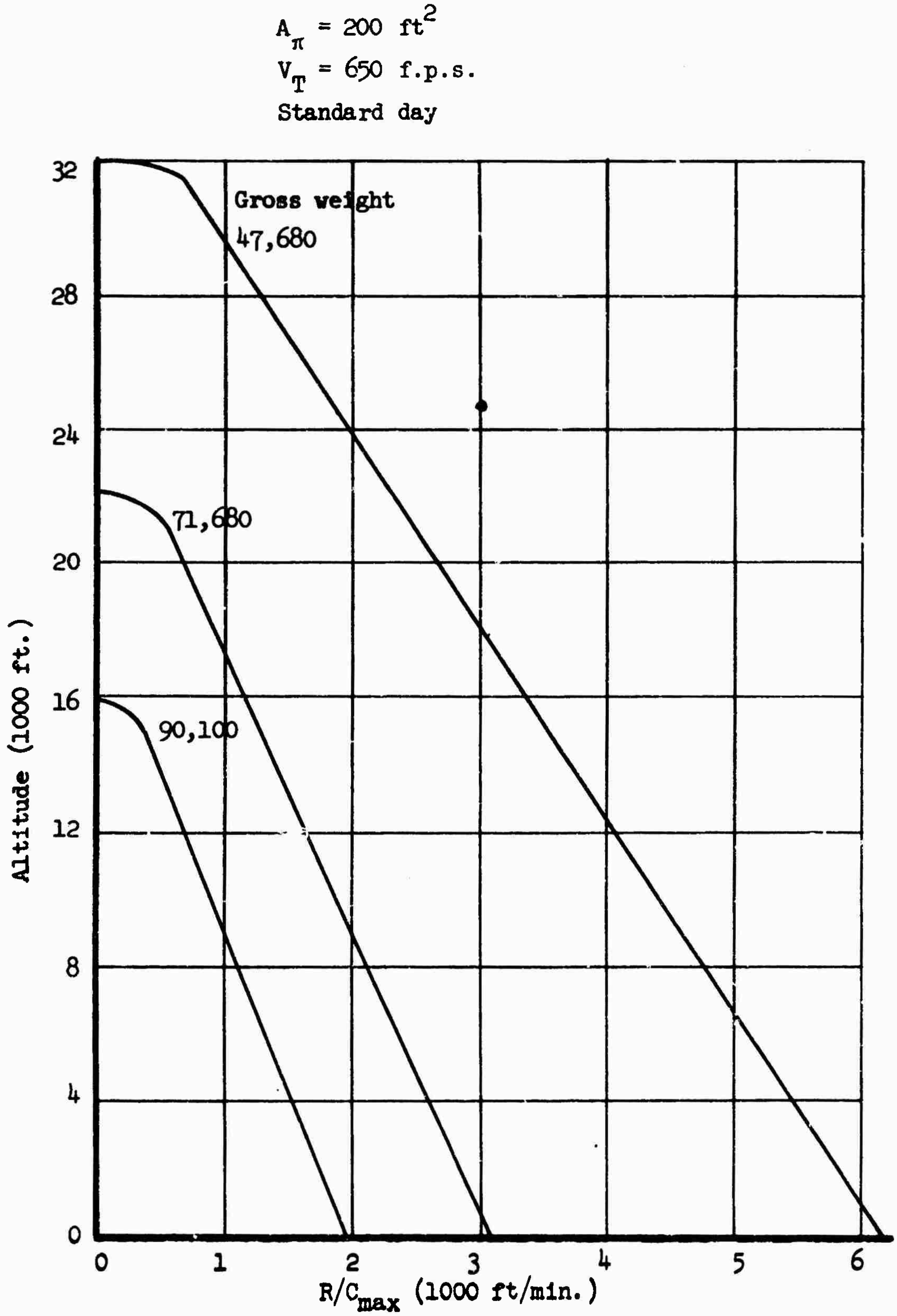

Figure 26. Maximum Rate of Climb Versus Altitude at Military Rated Power.

$A_\pi = 200\ ft^2$
$V_T = 650$ f.p.s.
Standard day

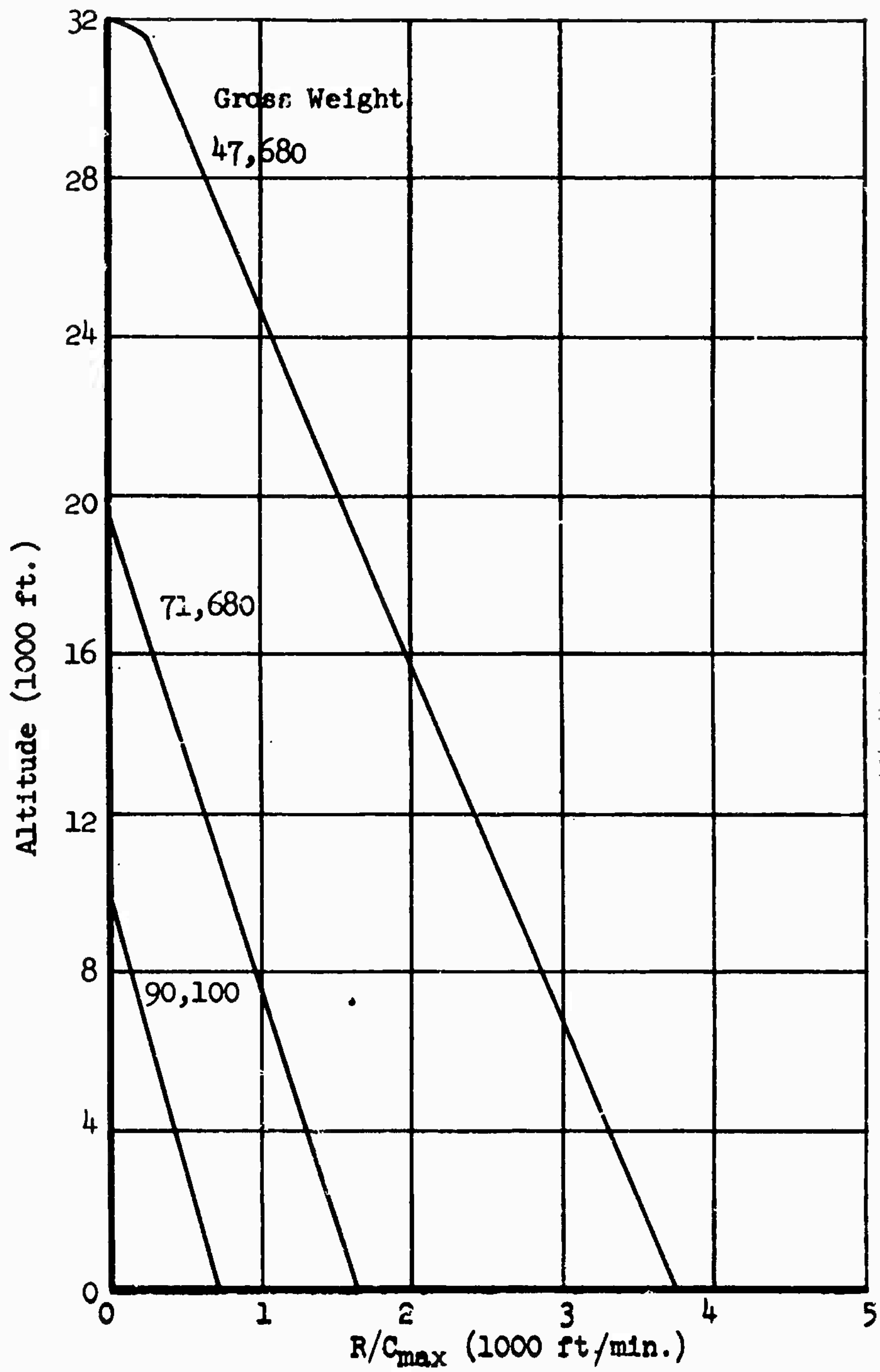

Figure 27. Maximum Rate of Climb Versus Altitude at Normal Rated Power.

$A_\pi = 200\ ft^2$
$v_T = 650$ f.p.s.
Standard day

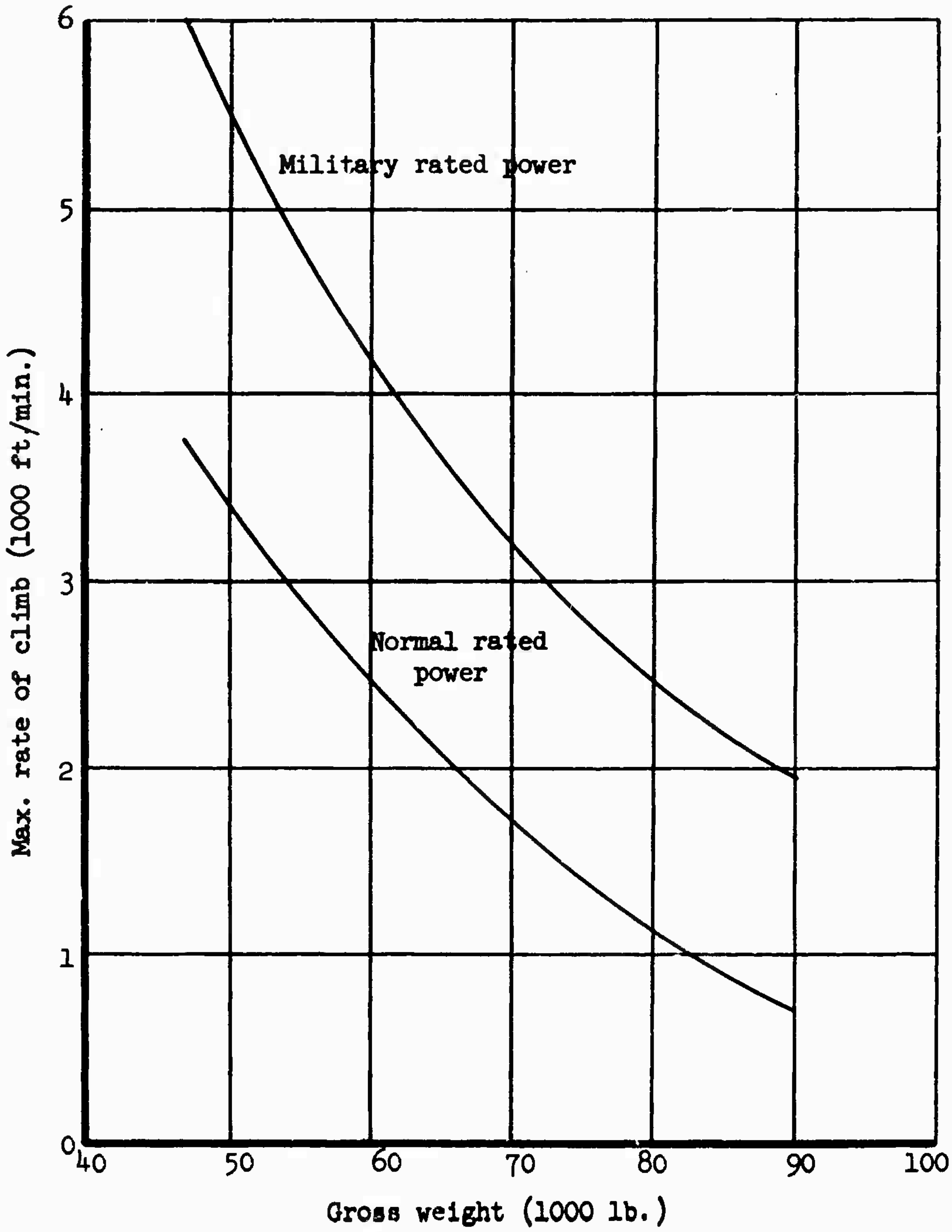

Figure 28. Maximum Rate of Climb Versus Gross Weight - Sea Level.

power required versus altitude for the selected speed points. The power required at the desired altitude can then be read from the cross-plot and the power available obtained from engine power curve, Figure 12. The difference between these two values is then the allowable climb power; the rate of climb is calculated as before by Equation (32).

6.2.2 Service Ceiling

Service ceiling by definition is the altitude at which the rate of climb is 100 f.p.m. The service ceiling was therefore determined from the maximum rate of climb versus altitude plots, Figures 26 and 27, at R/C_{max} = 100 f.p.m., and plotted versus gross weight in Figure 29. Service ceiling, like maximum rate of climb, is retreating blade compressibility limited at all gross weights.

6.2.3 Vertical Rate of Climb

Vertical rate of climb is calculated by the method of Reference 3. This method is based on momentum theory and relates vertical rate of climb, induced velocity in climb, u_c, and induced velocity in hover, u_H.

The total flow through the rotor during vertical climb is

$$U_c = R/C_v + u_c \tag{33}$$

and the induced velocity in climb is

$$u_c = \frac{-R/C_v}{2} + \left[\frac{(R/C_v)^2}{4} + u_H^2\right]^{\frac{1}{2}} \tag{34}$$

From momentum theory

$$U_c = \frac{550 \text{ chp}}{1.13W} \tag{35}$$

The power available to produce this flow through the rotor in climb is

$$\text{chp} = (\eta)\text{ahp} - \text{Rhp}_H - \text{hp}_{acc} \tag{36}$$

Substituting Equations (34) and (35) in Equation (33) and solving for the vertical rate of climb, R/C_v,

$$R/C_v = 60\left(U_c - \frac{u_H^2}{U_c}\right) \tag{37}$$

Presented in Figures 30 and 31 are plots of vertical rate of climb versus altitude at selected gross weights for both normal and military power. The sea level data is cross-plotted in Figure 32 to yield curves of vertical rate of climb versus gross weight at normal and military rated power.

$A_\pi = 200\ ft^2$
$V_T = 650$ f.p.s.
Standard day

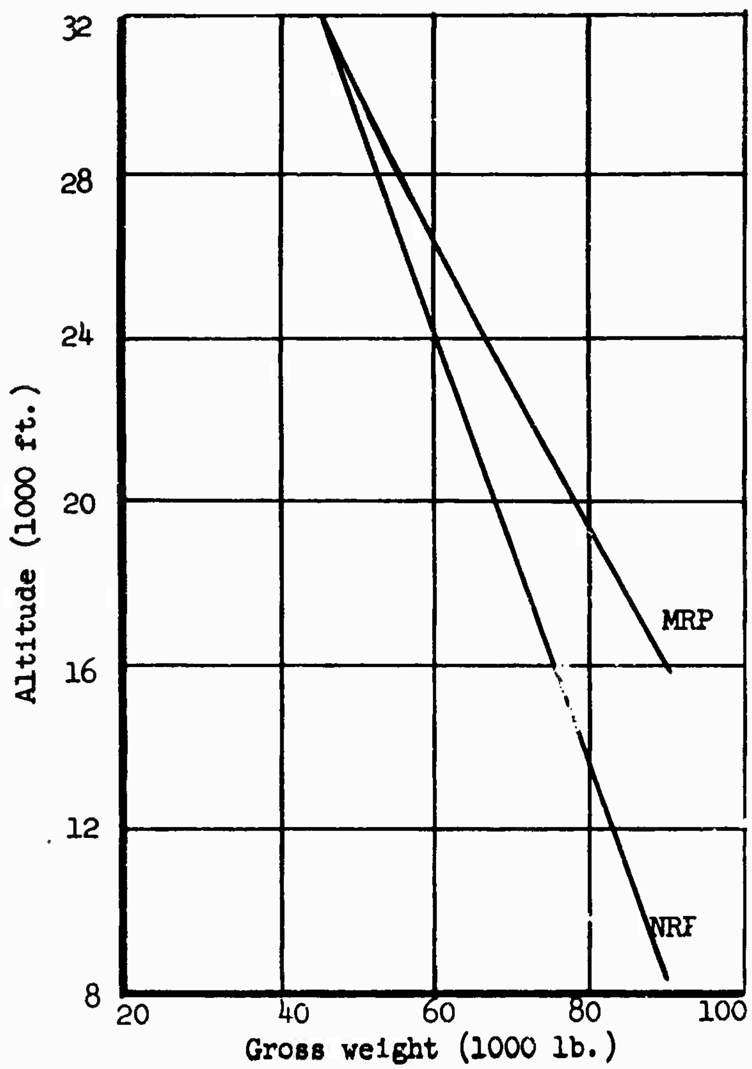

Figure 29. Service Ceiling Versus Gross Weight.

Sample calculation: Vertical rate of climb, sea level at 71,680 pounds.

$ahp = 14{,}500$ hp (NRP, Figure 12)

$\eta = .97$ at $V = 0$ (Section 4.6)

$Rhp_H = 3477$ hp (Paragraph 4.2)

$hp_{acc} = 100$ hp (Paragraph 4.4)

$$u_H = \frac{1.13}{.97}\sqrt{\frac{7.3}{2(.00238)}} = 40.4 \text{ f.p.s.} \qquad \text{(Equation (6)}$$

$$chp = .97(14{,}575) - 3{,}477 - 100 = 10{,}573 \qquad \text{(Equation(36)}$$

$$U_c = \frac{550(10{,}573)}{1.13(71{,}680)} = 71.8 \text{ f.p.s.} \qquad \text{(Equation (35)}$$

$$R/C_v = 60\left[71.8 \ \frac{(40.4)^2}{71.8}\right] = 2{,}940 \text{ ft/min.} \qquad \text{(Equation (37)}$$

V_T = 650 f.p.s.
Standard day

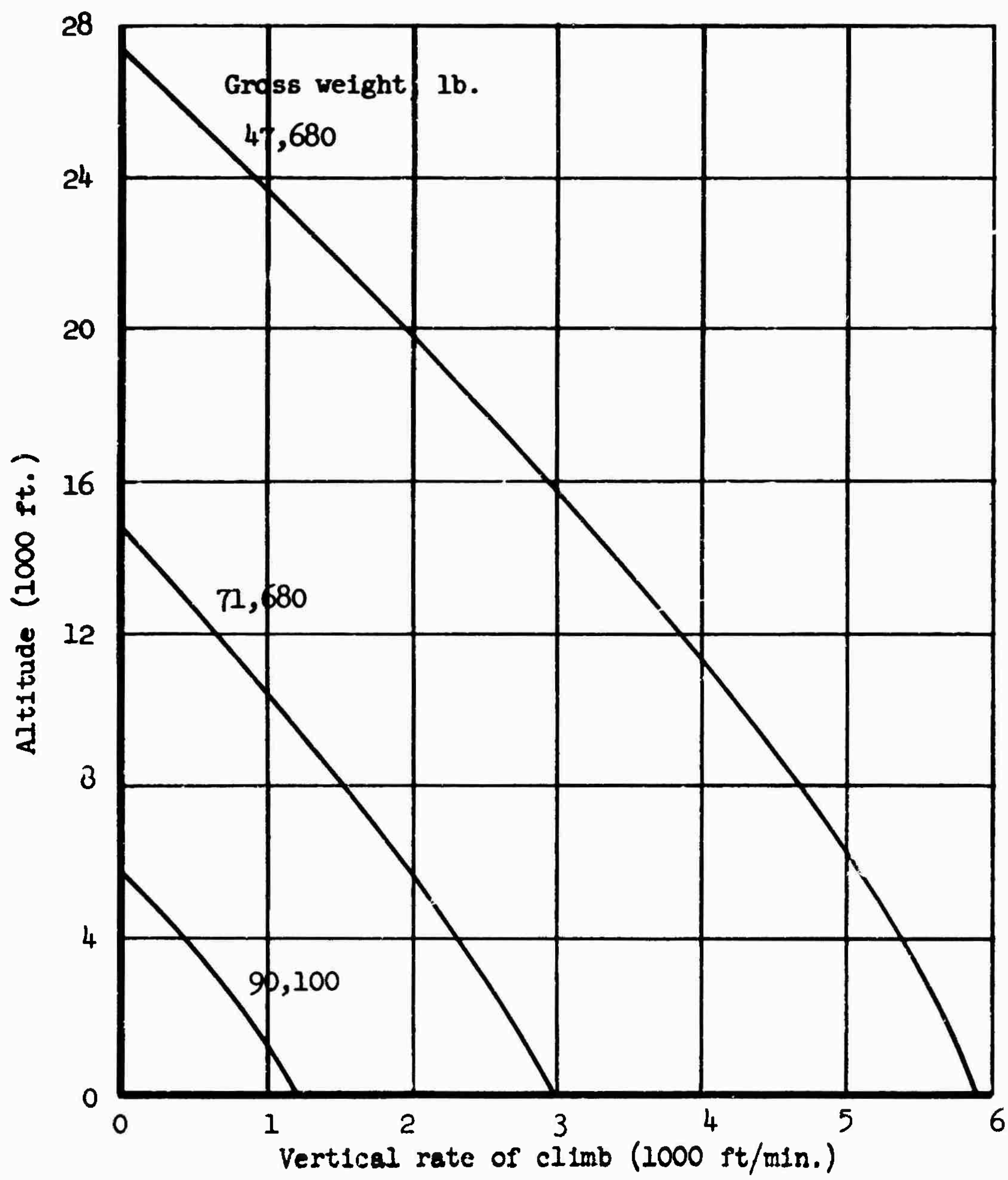

Figure 30 Vertical Rate of Climb Versus Altitude at Military Rated Power.

V_T = 650 f.p.s.
Standard day

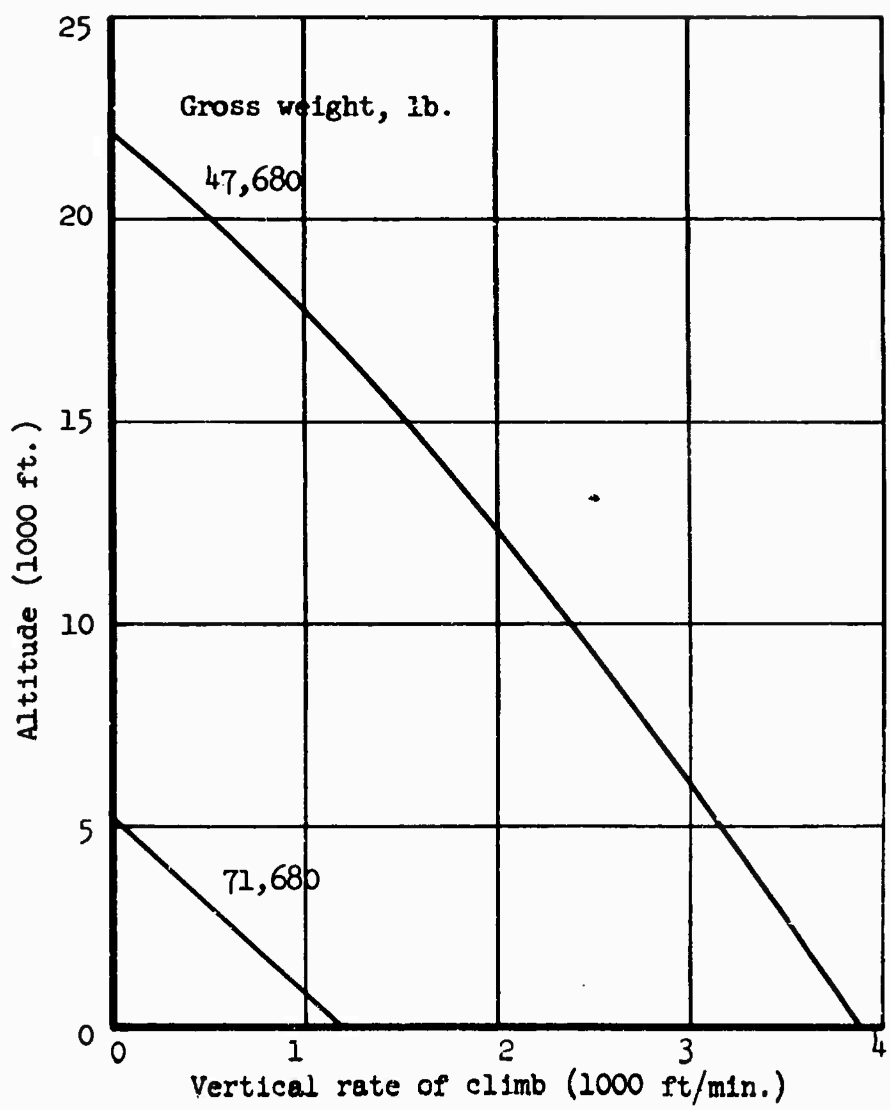

Figure 31. Vertical Rate of Climb Versus Altitude at Normal Rated Power.

V_T = 650 f.p.s.
Standard day

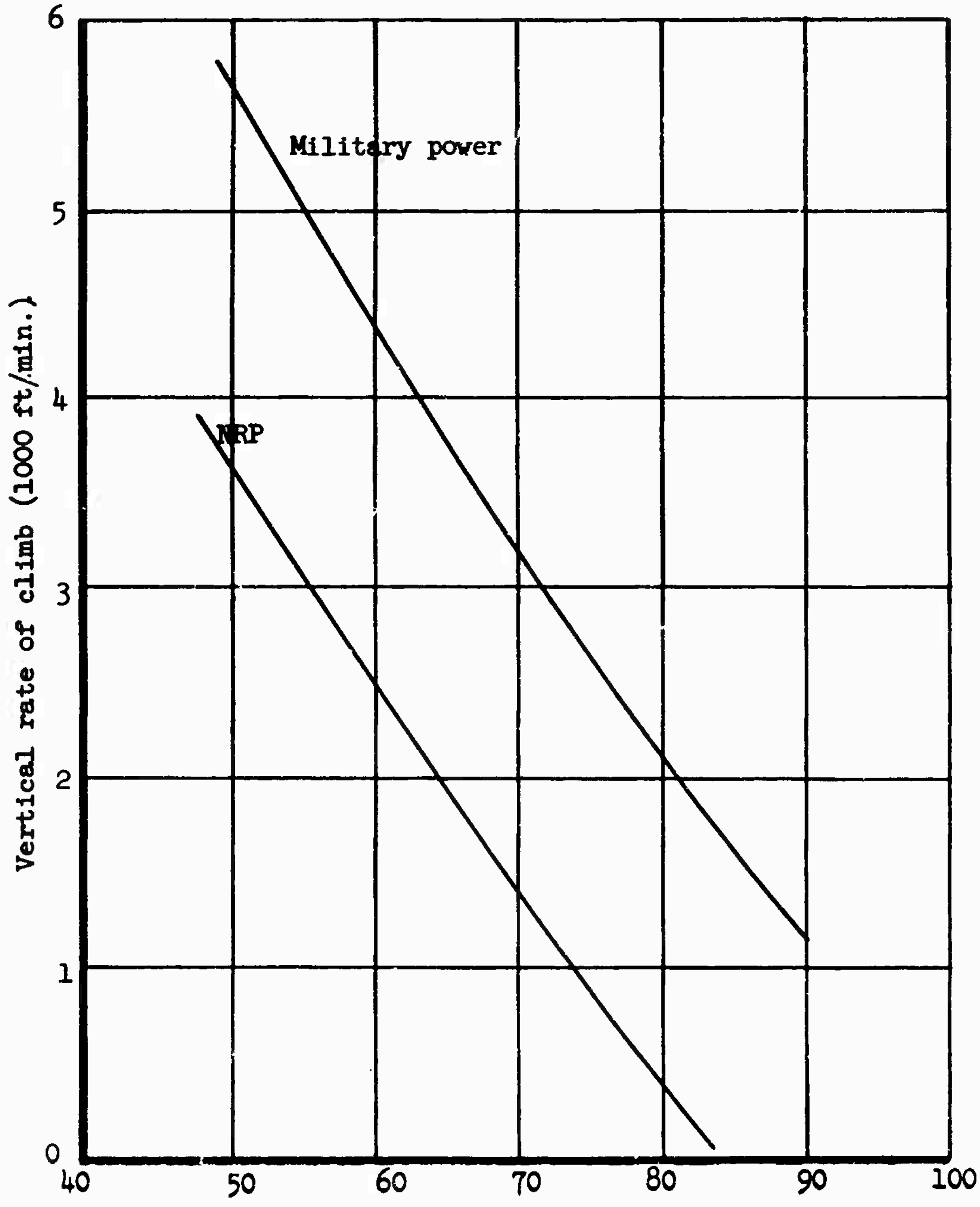

Figure 32. Vertical Rate of Climb Versus Gross Weight at Sea Level.

7.0 REFERENCES

1. "Airfoil Section Data Obtained in the NACA Variable Density Tunnel as Affected by Support Interference and Other Corrections," NACA Report No. 669, 1939.

2. United States Army Transportation Research Command* Contract No. DA 44-177-AMC-25(T).

3. Wiesner, Wayne A., "A Chart Method for Calculating Helicopter Performance and Parameters," Kellett Aircraft Corporation Report No. 130-9, Willow Grove, Pa., date unknown.

4. "Performance Data Report," Proposal for the Light Observation Helicopter (Army), Hiller Aircraft Engineering Report No. 60-92, Hiller Aircraft Company, Inc., Palo Alto, California, December 1960.

5. "Continental Model 357-1 Tip Turbojet Engine - Preliminary Model Specification," Heavy-Lift Tip Turbojet Rotor System, Volume XIII, CAE Model Specification No. 2253, U. S. Army Transportation Research Command,* Fort Eustis, Virginia, October 1965.

6. Gessow and Myers, Aerodynamics of the Helicopter, The MacMillan Company, New York, N. Y., 1952.

7. "Parametric Design Study," Heavy-Lift Tip Turbojet Rotor System, Volume II, Hiller Engineering Report No. 64-42, U. S. Army Transportation Research Command,* Fort Eustis, Virginia, October 1965.

*Changed to U. S. Army Aviation Materiel Laboratories in March 1965.

Unclassified

Security Classification

DOCUMENT CONTROL DATA - R&D

(Security classification of title, body of abstract and indexing annotation must be entered when the overall report is classified)

1. ORIGINATING ACTIVITY (Corporate author) Hiller Aircraft Company, Inc. Palo Alto, California	2a. REPORT SECURITY CLASSIFICATION Unclassified 2b GROUP

3. REPORT TITLE

Heavy-Lift Tip Turbojet Rotor System, "Performance Analysis", Volume IX

4. DESCRIPTIVE NOTES (Type of report and inclusive dates)

5. AUTHOR(S) (Last name, first name, initial)

6. REPORT DATE	7a. TOTAL NO. OF PAGES	7b. NO. OF REFS
October 1965	64	7

8a. CONTRACT OR GRANT NO. DA 44-177-AMC-25(T) b. PROJECT NO. c. Task 1M121401D14412 d.	9a. ORIGINATOR'S REPORT NUMBER(S) USAAVLABS Technical Report 64-68I 9b. OTHER REPORT NO(S) (Any other numbers that may be assigned this report) Hiller Engineering Report No. 64-49

10. AVAILABILITY/LIMITATION NOTICES

Qualified requesters may obtain copies of this report from DDC.
This report has been furnished to the Department of Commerce for sale to the public.

11. SUPPLEMENTARY NOTES	12. SPONSORING MILITARY ACTIVITY US Army Aviation Materiel Laboratories Fort Eustis, Virginia

13. ABSTRACT

Volume IX of a report on the heavy-lift tip turbojet rotor system presents a performance and characteristics summary of the Model 1108 tip turbojet-powered heavy-lift helicopter. The configuration was selected from a parametric analysis (USAAVLABS Technical Report 64-68B). Standard performance methods are used modified where necessary by factors peculiar to tip turbojet propulsion.

DD FORM 1 JAN 64 1473

Unclassified

Security Classification

Unclassified

Security Classification

14. KEY WORDS	LINK A		LINK B		LINK C	
	ROLE	WT	ROLE	WT	ROLE	WT
Tip Turbojet Rotor System Performance Analysis						

INSTRUCTIONS

1. ORIGINATING ACTIVITY: Enter the name and address of the contractor, subcontractor, grantee, Department of Defense activity or other organization (*corporate author*) issuing the report.

2a. REPORT SECURITY CLASSIFICATION: Enter the overall security classification of the report. Indicate whether "Restricted Data" is included. Marking is to be in accordance with appropriate security regulations.

2b. GROUP: Automatic downgrading is specified in DoD Directive 5200.10 and Armed Forces Industrial Manual. Enter the group number. Also, when applicable, show that optional markings have been used for Group 3 and Group 4 as authorized.

3. REPORT TITLE: Enter the complete report title in all capital letters. Titles in all cases should be unclassified. If a meaningful title cannot be selected without classification, show title classification in all capitals in parenthesis immediately following the title.

4. DESCRIPTIVE NOTES: If appropriate, enter the type of report, e.g., interim, progress, summary, annual, or final. Give the inclusive dates when a specific reporting period is covered.

5. AUTHOR(S): Enter the name(s) of author(s) as shown on or in the report. Enter last name, first name, middle initial. If military, show rank and branch of service. The name of the principal author is an absolute minimum requirement.

6. REPORT DATE: Enter the date of the report as day, month, year; or month, year. If more than one date appears on the report, use date of publication.

7a. TOTAL NUMBER OF PAGES: The total page count should follow normal pagination procedures, i.e., enter the number of pages containing information.

7b. NUMBER OF REFERENCES: Enter the total number of references cited in the report.

8a. CONTRACT OR GRANT NUMBER: If appropriate, enter the applicable number of the contract or grant under which the report was written.

8b, 8c, & 8d. PROJECT NUMBER: Enter the appropriate military department identification, such as project number, subproject number, system numbers, task number, etc.

9a. ORIGINATOR'S REPORT NUMBER(S): Enter the official report number by which the document will be identified and controlled by the originating activity. This number must be unique to this report.

9b. OTHER REPORT NUMBER(S): If the report has been assigned any other report numbers (*either by the originator or by the sponsor*), also enter this number(s).

10. AVAILABILITY/LIMITATION NOTICES: Enter any limitations on further dissemination of the report, other than those imposed by security classification, using standard statements such as:

(1) "Qualified requesters may obtain copies of this report from DDC."

(2) "Foreign announcement and dissemination of this report by DDC is not authorized."

(3) "U. S. Government agencies may obtain copies of this report directly from DDC. Other qualified DDC users shall request through ______."

(4) "U. S. military agencies may obtain copies of this report directly from DDC. Other qualified users shall request through ______."

(5) "All distribution of this report is controlled. Qualified DDC users shall request through ______."

If the report has been furnished to the Office of Technical Services, Department of Commerce, for sale to the public, indicate this fact and enter the price, if known.

11. SUPPLEMENTARY NOTES: Use for additional explanatory notes.

12. SPONSORING MILITARY ACTIVITY: Enter the name of the departmental project office or laboratory sponsoring (*paying for*) the research and development. Include address.

13. ABSTRACT: Enter an abstract giving a brief and factual summary of the document indicative of the report, even though it may also appear elsewhere in the body of the technical report. If additional space is required, a continuation sheet shall be attached.

It is highly desirable that the abstract of classified reports be unclassified. Each paragraph of the abstract shall end with an indication of the military security classification of the information in the paragraph, represented as *(TS), (S), (C),* or *(U)*.

There is no limitation on the length of the abstract. However, the suggested length is from 150 to 225 words.

14. KEY WORDS: Key words are technically meaningful terms or short phrases that characterize a report and may be used as index entries for cataloging the report. Key words must be selected so that no security classification is required. Identifiers, such as equipment model designation, trade name, military project code name, geographic location, may be used as key words but will be followed by an indication of technical context. The assignment of links, rules, and weights is optional.

Unclassified

Security Classification